



ATTI  
DELLA  
SOCIETÀ TOSCANA  
DI  
SCIENZE NATURALI

MEMORIE • SERIE A • VOLUME CXXIV • ANNO 2017



Edizioni ETS



MUSEO DI STORIA NATURALE

Con il contributo del Museo di Storia Naturale dell'Università di Pisa



e della Fondazione Cassa di Risparmio di Lucca

## INDICE - CONTENTS

<p>C. BIAGIONI, Y. MOËLO, F. ZACCARINI, Ferdowsiite from the Monte Arsiccio mine, Apuan Alps, Tuscany (Italy): occurrence and crystal structure. <i>Ferdowsiite della miniera di Monte Arsiccio, Alpi Apuane, Toscana (Italia): giacitura e struttura cristallina.</i></p>	<p>pag. 5</p>	<p><i>Broadkill Beach Delaware: caso di studio di un progetto per un uso vantaggioso di materiale dragato.</i></p>	<p>» 83</p>
<p>C. BIAGIONI, S. MUSETTI, M. PASERO, New data on metacinnabar from Tuscany (Italy). <i>Nuovi dati sul metacinnabro toscano.</i></p>	<p>» 13</p>	<p>J. GUILLÉN, G. SIMARRO, A. CORAL, Morphological changes in the artificially embayed beaches of the Barcelona City (Spain). <i>Variazioni morfologiche delle spiagge artificiali della città di Barcellona (Spagna).</i></p>	<p>» 93</p>
<p>P. BILLI, Quantification of bedload flux to beaches within a global change perspective. <i>Stima degli apporti solidi fluviali alle spiagge in una prospettiva di cambiamento globale.</i></p>	<p>» 19</p>	<p>M. LUPPICHINI, M. BINI, R. GIANNECCHINI, Evoluzione temporale del sedime edilizio nella Versilia pre-alluvione 1996 in rapporto alle mappe di pericolosità idraulica e da frana mediante <i>software GIS open source e open data.</i></p>	<p>» 101</p>
<p>P. BILLI, Hydro-morphology of discontinuous gullies: an Ethiopian example. <i>Idromorfologia dei solchi d'erosione discontinui: un esempio Etiopico.</i></p>	<p>» 31</p>	<p>F. RAPETTI, Tendenze attuali della temperatura dell'aria presso i laghi artificiali di Chiotas, Serrù, Goillet e Gabiet, nella media montagna delle Alpi Marittime, Graie e Pennine Italiane. <i>Air temperature trends by the artificial lakes of Chiotas, Serrù, Goillet and Gabiet, in a medium-altitude mountain environment in the Maritime, Graian and Pennine Alps, in Italy.</i></p>	<p>» 115</p>
<p>M. BOSSELAERS, F. VAN NIEULANDE, A. COLLARETA, A new record of <i>Cetopirus complanatus</i> (Cirripedia: Coronulidae), an epibiont of right whales (Cetacea: Balaenidae: <i>Eubalaena</i> spp.), from a beach deposit of Mediterranean Spain. <i>Nuova segnalazione di Cetopirus complanatus (Cirripedia: Coronulidae), un epibionte delle balene franche (Cetacea: Balaenidae: Eubalaena spp.), da un deposito di spiaggia della costa Mediterranea della Spagna.</i></p>	<p>» 43</p>	<p>G. SARTI, D. BERTONI, M. CAPITANI, A. CIAMPALINI, L. CIULLI, A. C. FERONI, S. ANDREUCCI, G. ZANCHETTA, I. ZEMBO, Facies analysis of four superimposed Transgressive-Regressive sequences formed during the two last interglacial-glacial cycles (central Tuscany, Italy). <i>Analisi di facies di quattro sequenze trasgressivo-regressive (T-R) sovrapposte, formate durante gli ultimi due cicli interglaciale-glaciale (Toscana centrale, Italia).</i></p>	<p>» 133</p>
<p>A. COLLARETA, S. CASATI, A. DI CENCIO, A pristinid sawfish from the lower Pliocene of Lucciolabella (Radicofani basin, Tuscany, central Italy). <i>Un pesce sega della famiglia Pristidae dal Pliocene inferiore di Lucciolabella (Bacino di Radicofani, Toscana, Italia centrale).</i></p>	<p>» 49</p>	<p>M. SIMONETTI, R. CAROSI, C. MONTOMOLI, Variscan shear deformation in the Argentera Massif: a field guide to the excursion in the Pontebernardo Valley (Cuneo, Italy). <i>Deformazione non coassiale Varisca nel Massiccio dell'Argentera: guida all'escursione nel Vallone di Pontebernardo (Cuneo, Italia).</i></p>	<p>» 151</p>
<p>G. CRUCIANI, D. FANCELLO, M. FRANCESCHELLI, G. MUSUMECI, The Paleozoic basement of Monte Grighini Unit, a deep view in the nappe structure of Variscan belt in Sardinia. Synthesis of geological data and field guide. <i>Il basamento Paleozoico dell'Unità del Monte Grighini, uno sguardo approfondito nella struttura delle falde della catena Varisca Sarda. Sintesi dei dati geologici e guida all'escursione.</i></p>	<p>» 57</p>	<p>Processi Verbali - <a href="http://www.stsn.it">http://www.stsn.it</a></p>	<p>» 171</p>
<p>S. DOHNER, A. TREMBANIS, Broadkill Beach Delaware: case study of a beneficial use of dredged material project.</p>			



GABRIELE CRUCIANI <sup>(\*)</sup>, DARIO FANCELLO <sup>(\*)</sup>, MARCELLO FRANCESCHELLI <sup>(\*)</sup>, GIOVANNI MUSUMECI <sup>(\*\*)</sup>

# THE PALEOZOIC BASEMENT OF MONTE GRIGHINI UNIT, A DEEP VIEW IN THE NAPPE STRUCTURE OF VARISCAN BELT IN SARDINIA. SYNTHESIS OF GEOLOGICAL DATA AND FIELD GUIDE

**Abstract** - G. CRUCIANI, D. FANCELLO, M. FRANCESCHELLI, G. MUSUMECI, *The Paleozoic basement of Monte Grighini Unit, a deep view in the nappe structure of Variscan belt in Sardinia. Synthesis of geological data and field guide.*

The Monte Grighini Complex (MGC; central-west Sardinia) is a metamorphic complex belonging to the Nappe Zone of the Sardinian Variscan belt, located at the northwestern end of the Flumendosa Antiform. It consists of three tectonic units, among which Monte Grighini Unit represent the deepest of the whole nappe zone, and a kilometer-wide shear zone with synkinematic granitoid intrusion. We present a guide for a two days field trip. The first day will be mainly focused on the metamorphic rocks of Monte Grighini Unit, and mylonitic leucogranite with S-C fabric together with other interesting structures (i.e. a giant quartz dyke). The second day will be developed along the mylonite/cataclaste belt on the southwestern side of the complex. The field guide is preceded by a brief, updated *excursus* on Sardinian Variscan basement and by a detailed description of the complex from the most recent papers.

**Key words** - Monte Grighini metamorphic units; shear zone; ultramylonite; synkinematic granitoids; Variscan orogeny; Sardinia

**Riassunto** - G. CRUCIANI, D. FANCELLO, M. FRANCESCHELLI, G. MUSUMECI, *Il basamento Paleozoico dell'Unità del Monte Grighini, uno sguardo approfondito nella struttura delle falde della catena Varisca Sarda. Sintesi dei dati geologici e guida all'escursione.*

Il complesso del Monte Grighini (MGC; Sardegna centro-occidentale) è un complesso metamorfico appartenente alla Zona a Falde della catena Varisca Sarda. Esso è situato all'estremità nord-occidentale dell'antiforme del Flumendosa ed è costituito da tre unità tettoniche sovrapposte, tra le quali l'Unità del Monte Grighini rappresenta la più profonda dell'intera zona a falde, e da una zona di taglio chilometrica marcata dall'intrusione di granitoidi sincinemati. Di seguito viene presentata una guida all'escursione articolata in due giorni. Il primo giorno sarà incentrato prevalentemente sull'unità metamorfica del Monte Grighini e su un leucogranito milonitico con strutture S-C insieme ad altre interessanti strutture quali un filone di quarzo chilometrico. Il secondo giorno si svilupperà lungo la fascia milonitica/cataclastica affiorante lungo il margine sud-occidentale del complesso. La guida all'escursione sarà preceduta da un breve e aggiornato *excursus* sul basamento Varisco Sardo e da una dettagliata descrizione del complesso del Monte Grighini emergente dalla più recente letteratura.

**Parole chiave** - Unità metamorfiche del Monte Grighini; zona di taglio; ultramilonite; granitoidi sincinemati; orogenesi Varisca; Sardegna

## INTRODUCTION

The Paleozoic basement of Sardinia is a classical collisional-type chain made up of an External Zone (SW Sardinia), a Nappe zone (central Sardinia) and an Axial Zone (north Sardinia) (Carmignani *et al.*, 1994, 2001). Since the seventies the Variscan chain of Sardinia has been the subject of several geological studies that have defined the structure, the tectono-metamorphic evolution and the sequence of volcanic and intrusive cycles (Carmignani *et al.*, 1994, 2001; Franceschelli *et al.*, 2005a; Cruciani *et al.*, 2015c).

The most relevant features of the Sardinia chain are the slight increase of the degree of metamorphism from the External to Nappe Zone opposed to the rapid increase of metamorphic grade in the Axial Zone. In the Axial Zone, the P-T paths of eclogite, chloritoid-bearing schist, and migmatite have allowed to characterize the tectono-metamorphic evolution, the main geodynamic processes during the Variscan orogeny, and their main relationships with other terranes of the southern European Variscides (Carosi & Palmeri, 2002; Ricci *et al.*, 2004; Carosi *et al.*, 2012, 2015; Cruciani *et al.*, 2010, 2015a,b; Massonne *et al.*, 2013). In the Nappe Zone the metamorphic rocks show a slight metamorphic zonation from south to north and from the lower (Mt. Grighini) to the upper unit (Gerrei Unit).

The Monte Grighini Unit, the deepest portion of the Nappe zone, outcropping in the core of the Flumendosa antiform, is bounded by one of the main late Variscan strike-slip shear zones (Elter *et al.*, 1990; Musumeci, 1992; Musumeci *et al.*, 2015; Cruciani *et al.*, 2016).

Based on the lithological composition, metamorphism and on the occurrence of several types of granitoids, the Monte Grighini Unit constitutes the main element of correlation for the tectono-metamorphic evolution of the metasedimentary sequences between the Axial Zone and the various tectonic units of the Nappe Zone. The aim of this paper is to provide an overview of geological and petrological data of the rocks of the Mon-

<sup>(\*)</sup> Dipartimento di Scienze Chimiche e Geologiche, Università di Cagliari, Via Trentino 51, I-09127, Cagliari, Italy

<sup>(\*\*)</sup> Dipartimento di Scienze della Terra, Università di Pisa, Via Santa Maria 53, I-56126, Pisa, Italy. Corresponding author, E-mail: gm@dst.unipi.it

te Grighini Unit and their geological interpretations within a regional scale framework.

This paper is accompanied by a geological field guide through the most representative outcrops of the Monte Grighini Unit that delineate the tectono-metamorphic evolution and the character of igneous intrusive rocks in the root of the Variscan Nappe Zone of Sardinia.

#### GEOLOGICAL FRAME OF THE VARISCAN CHAIN

The Paleozoic basement of Sardinia belongs to the European Variscan chain. Together with Corsica it is usually correlated with Maures (Elter *et al.*, 1990, 1999, 2010; Elter & Pandeli, 2005; Corsini & Rolland, 2009). After Carmignani *et al.* (1994, 2001) the Sardinian segment of the Variscan chain is divided into four tectono-metamorphic zones. From NE to SW

they are (Fig. 1): 1) Axial zone, with medium- to high-grade metamorphic rocks and migmatites. Metabasite lenses, with eclogite and granulite-facies relics, occur in the migmatites; 2) Internal Nappe zone, with low- to medium-grade metamorphic rocks; 3) External Nappe zone, with low-grade metamorphic rocks; 4) External zone, with very low- to low-grade metamorphic rocks.

*The Axial Zone* - The Axial (or Inner) Zone corresponds to northern Sardinia (Fig. 1) and consists of medium to high-grade metamorphic rocks, intruded by late Carboniferous-Permian igneous rocks. This zone was further subdivided into two metamorphic complexes, separated by a major shear zone, the Posada-Asinara Line (PAL; Carmignani *et al.*, 1994, 2001; Carosi & Oggiano, 2002; Carosi & Palmeri, 2002; Helbing, 2003; Padovano *et al.*, 2012; Carosi *et al.*, 2005, 2012, 2015). The High-Grade Metamorphic Complex (HGMC), north of the PAL, is made up of gneisses and igneous- and sed-

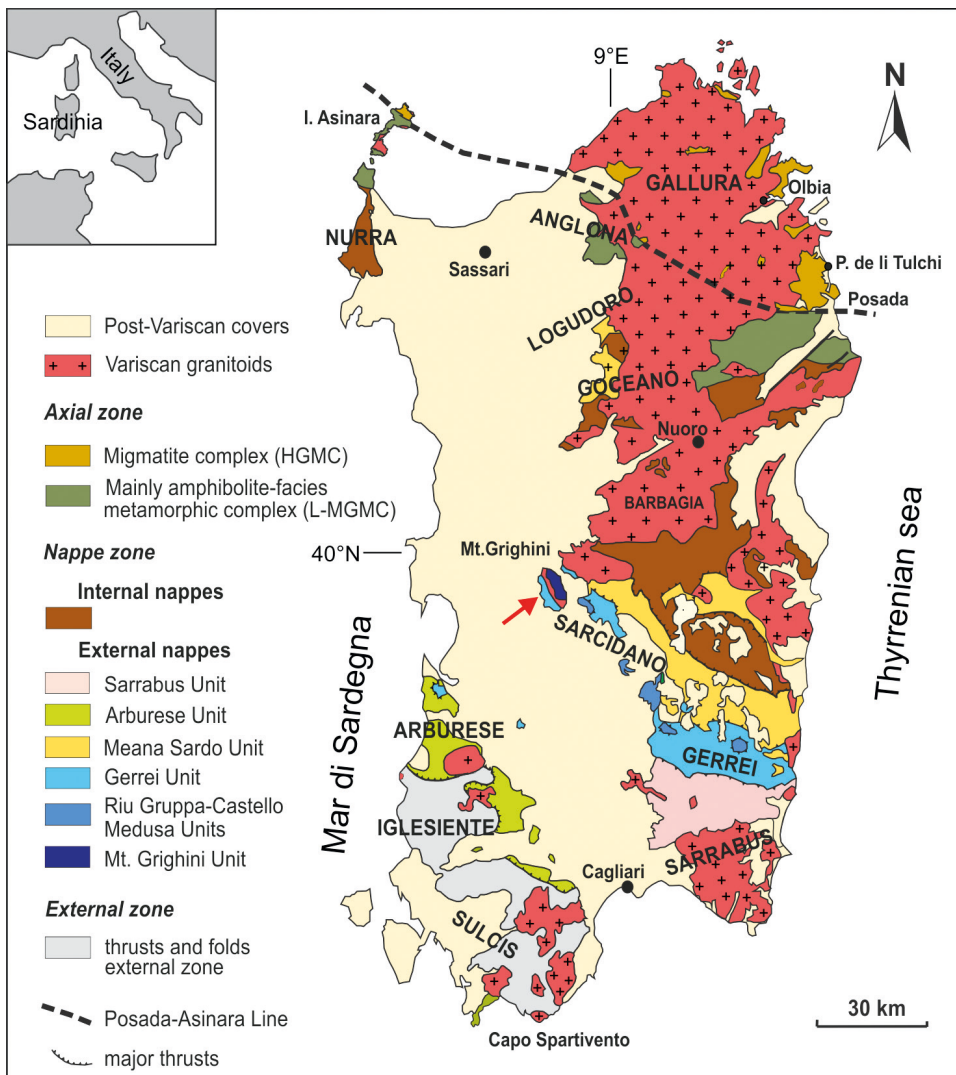


Fig. 1 - Tectonic sketch map of the Variscan Belt of Sardinia (modified from Carmignani *et al.*, 2001). The red arrow shows the location of the Monte Grighini Metamorphic Complex.

imentary-derived migmatites (Cruciani *et al.*, 2008a,b, 2014a,b; Massonne *et al.*, 2013). It is also characterized by minor calc-silicate nodules, gneiss, metabasite lenses still preserving granulite (Ghezzi *et al.*, 1979; Franceschelli *et al.*, 2002) and/or eclogite-facies relics (Miller *et al.*, 1976; Franceschelli *et al.*, 2007; Cruciani *et al.*, 2011, 2012), and mafic-silicic layered sequences resembling leptyno-amphibolite complexes that are preserved within the migmatites (Franceschelli *et al.*, 2005b). The Low to Medium Grade Metamorphic Complex (L-MG-MC), south of the PAL, consists of a sequence of mica-schists, para and orthogneisses (Carosi & Palmeri, 2002; Carosi *et al.*, 2005, 2015; Cruciani *et al.*, 2013a) and minor amphibolite lenses sometimes preserving eclogite-facies relics (Cruciani *et al.*, 2015a,b).

*The Nappe Zone*- it extends throughout the central part of the island (Fig. 1) and is characterized by a stack of southward verging tectonic units. Based on stratigraphic, structural and metamorphic differences, this zone is further divided into External and Internal Nappe Zone (Carmignani *et al.*, 1994; Conti *et al.*, 2001).

The Internal Nappe Zone consists of metasandstones, quartzites and phyllites in the Monti del Gennargentu ("Postgotlandiano "Auct. p.p"), Goceano and Nurra regions. Additionally, metaconglomerates crop out in Goceano, Barbagia and Baronia near to the contact with metavolcanic rocks. Micaschists and paragneisses belonging to the internal units crop out in Barbagia and Baronia. Acidic metavolcanic rocks, known in the literature as "Porfiroidi", metarkoses and microcline-bearing quartzites, together with subordinate mafic and intermediate (andesite) metavolcanic rocks of probable Middle-Ordovician age are also found in the Internal Nappes (Oggiano *et al.*, 2010; Gaggero *et al.*, 2012). These rocks are followed by Siluro-Devonian graphite-rich black phyllite, marble and calcschist with small bodies of metadolerite and metagabbro of Lower Carboniferous age. The lithological sequences that crop out in southern Nurra and Baronia can be correlated with the Cambro-Ordovician successions of the External Zone.

The External Nappe Zone is characterized by the occurrence of thick metavolcanic sequences, related to a Middle Ordovician magmatism, cropping out above Cambro-Ordovician metapsammites. The sedimentary cycle started at the beginning of the Upper Ordovician (Caradoc), when a marine transgression occurred on the remains of a volcanic arc. Silurian black phyllites have an homogeneous areal distribution, which most likely corresponds to an extended pelagic environment, whereas Devonian carbonates, related to a platform environment, gradually decrease their thickness towards the inner parts of the chain. In the External Nappe Zone, the deepest metamorphic units are the Castello Medusa, Riu Gruppa and Monte Grighini Units, reaching the biotite zone and staurolite - sillimanite zone,

respectively. The metamorphic rocks of the Monte Grighini Unit, recently characterized in detail in their mineralogy, petrography, geochemistry and P-T conditions (Cruciani *et al.*, 2013b, 2016; Musumeci *et al.*, 2015) represent the core of the greatest tectonic culmination in the Nappe Zone (Carmignani *et al.*, 1994).

*The External Zone*-it corresponds to the southwestern part of Sardinia (Fig. 1). In southern Sulcis, the Cambro-Ordovician sequence includes, from bottom to top, Monte Settiballas micaschists, the Bithia Fm. and the Monte Filau orthogneiss (Carmignani *et al.*, 1994). The Bithia Fm. is made up of alternating metapsammites and metapelites, with metavolcanics and carbonate intercalations (Junker & Schneider, 1983). Some authors consider the Settiballas micaschists and Bithia Fm. as a part of a Precambrian to early Cambrian basement (Costamagna, 2015; Costamagna *et al.*, 2016) other authors consider the Bithia Fm. of Ordovician age (Pavanetto *et al.*, 2012). The Monte Filau orthogneiss are lower Ordovician granitoids (Delaperrière & Lancelot, 1989; Pavanetto *et al.*, 2012) intruded within Settiballas micaschists.

The Cambrian-Early Ordovician sequence is made up, from bottom to top, of the Nebida Group, Gonnese Group and Iglesias Group (Pillola, 1991). The Nebida Group is a deltaic terrigenous sequence (metasandstone and metasilite), with rare, interlayered, lagoon, oolitic limestones followed by the Gonnese Group that is interpreted as a thick platform carbonate succession showing gradual heteropic transition to nodular limestones (extensional deep basins). The Iglesias Group consists of nodular, crystalline, marly limestone at the base, and of phyllites and metasilites interbedded with subordinate massive fine-grained metasandstones at the top (Cabitza Fm).

A sharp angular unconformity known as the Sardinian phase, which is overlain by a transgressive (Martini *et al.*, 1991) polygenic metaconglomerate, namely the Pudding Auct., separates the Cambrian-Early Ordovician rocks from the overlying Upper Ordovician-Lower Carboniferous sedimentary cycle. The metasedimentary sequence of the External Zone ends with the deposits of Silurian and Devonian age, mainly consisting of carbonate, and the Pala Manna Fm. which represents the Variscan flysch (Carmignani *et al.*, 2001 and references therein).

#### VARISCAN TECTONO-METAMORPHIC FEATURES AND GEOCHRONOLOGICAL DATA IN THE AXIAL AND NAPPE ZONE

##### The Axial Zone

In the Axial Zone tectonic and metamorphic history of the two metamorphic complexes (HGMC and

L-MGMC) results from syn-collisional shortening marked by northward increase of deformation intensity and metamorphic grade. An early deformation ( $D_1$  phase) recognizable in the southern part of the Axial Zone is progressively transposed by a later deformation ( $D_2$  phase), moving toward the PAL at north (Carmignani *et al.*, 1994; Carosi & Palmeri, 2002). Metamorphic grade ranges from low metamorphic grade (upper greenschist facies) at south to high grade (migmatite-granulite facies) at north, with a fast increase in metamorphic grade in a restricted area of only ~40 km across which the following metamorphic zones were distinguished from south to north: 1) biotite; 2) garnet; 3) staurolite + biotite; 4) kyanite + biotite; 5) sillimanite; 6) sillimanite + K-feldspar i.e. migmatite zone (Franceschelli *et al.*, 1982; Connolly *et al.*, 1994). A high-pressure metamorphic event (1.8 GPa, 460-500°C), documented in chloritoid schist from the L-MGMC, was broadly coeval to the  $D_1$  deformation (Cruciani *et al.*, 2013a) and it was followed by a Barrovian-type metamorphism affecting the whole Axial Zone. The metamorphic units are widely intruded by Late Carboniferous-Early Permian granitoids of the Sardinian batholith which were in turn followed by the Late Carboniferous-Early Permian sedimentary basins (Barca *et al.*, 1995). A synoptic table of the

polyphase deformation, metamorphic evolution and magmatic events in the Axial Zone is shown in Fig. 2 (after Carosi *et al.*, 2015).

Metamorphic and radiometric data suggest the following sequence of Variscan events. An early phase of HP metamorphism, testified by some metabasites with eclogite relics embedded within the HGMC or L-MGMC, dated at 400±10 Ma by Palmeri *et al.* (2004), on the basis of U-Pb SHRIMP zircon data. A similar age of 403±4 Ma, interpreted as dating the high-grade event, was found by Cortesogno *et al.* (2004) for eclogites included in the HGMC. Giacomini *et al.* (2005) propose a Middle Ordovician protolith age for eclogites embedded within the Sardinian High-Grade Metamorphic Complex, an Early Visean age for eclogite facies metamorphism and a Late Visean age for amphibolite facies metamorphism, i.e. ages of 460-450 Ma, ~345 Ma and ~320 Ma, respectively. In the migmatitic rocks of the HGMC, old leucosome from a NE Sardinia migmatite yield an age of 344±7 Ma (Ferrara *et al.*, 1978, Rb/Sr whole rock). These ages indicate that partial melting and metasomatic processes started soon after the end of the  $D_1$  phase, with attainment of peak temperatures very close to the  $D_1$ - $D_2$  boundary. According to Ricci *et al.* (2004) and Elter *et al.* (1999) the age values around 350-344 Ma, (Del Moro *et al.*,

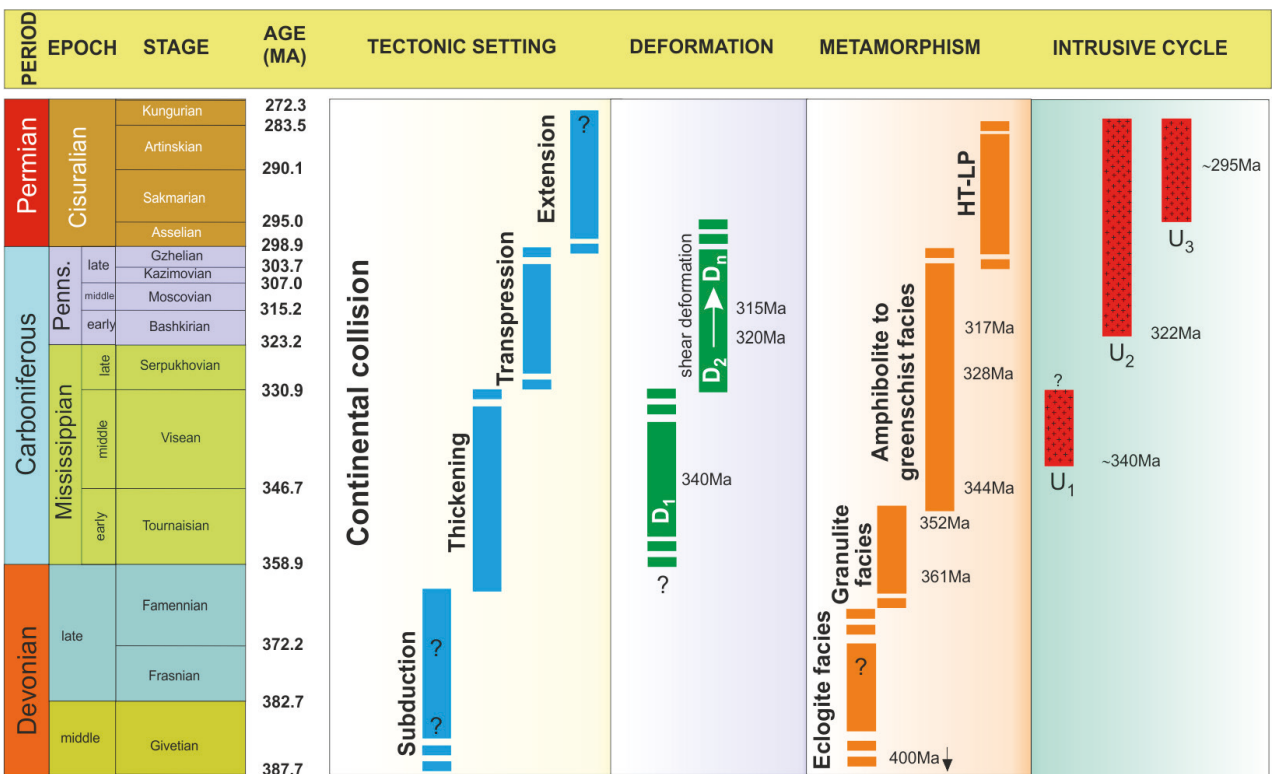


Fig. 2 - Synoptic table of the deformation, metamorphic and magmatic events in the Axial Zone of Sardinian Variscan basement. From Carosi *et al.* (2015) and Cruciani *et al.* (2015c).

1991a; Ferrara *et al.*, 1978) in the Axial Zone divided the end of collisional tectonics, with peak pressure attainment ( $D_1$  phase), from the beginning of the extensional tectonics, exhumation and uplift ( $D_2$  phase). In the L-MGMC, the Barrovian metamorphism coeval with the early thickening stage of the  $D_1$  event has been dated at 345-340 Ma (Di Vincenzo *et al.*, 2004). These ages are in agreement with (i) the Tournaisian age of syntectonic deposits (355-345 Ma) in the Nappe Zone of SE Sardinia and (ii) with an  $^{40}\text{Ar}$ - $^{39}\text{Ar}$  age of  $345\pm 4$  Ma on actinolite from a metagabbro (Del Moro *et al.*, 1991a). In particular in the garnet zone apparent  $^{40}\text{Ar}$ - $^{39}\text{Ar}$  ages of muscovite 340-335 Ma have been reported for syn- $D_1$  white mica and age clustering at 320-315 Ma for most syn- $D_2$  white mica (Di Vincenzo *et al.*, 2004). Based on syn- $D_2$  white mica Ar-Ar ages (Di Vincenzo *et al.*, 2004) and on monazite U-(Th)-Pb age (Carosi *et al.*, 2012), a reasonable age of ~320-315 Ma could be attributed to the  $D_2$  shear deformation along the PAL, the main tectonic structure in the Axial Zone. Furthermore, north of the PAL in the HGMC the coeval activity of large scale strike-slip shear zones controlled the emplacement and assembly of the main part of the Sardinian batholith between 312 and 308 Ma (Casini *et al.*, 2012, 2015). Barrovian mineral assemblages were overprinted by late Variscan (Rb-Sr age of  $303\pm 6$  Ma on muscovite, Del Moro *et al.*, 1991a) LP-HT parageneses related to gravitative collapse, exhumation and emplacement of intrusive granitoids at shallow crustal levels in the L-MGMC (Carmignani *et al.*, 1994; Casini & Oggiano, 2008).

### The Nappe Zone

In the Nappe Zone Variscan tectonics led to regional thrusting with km-scale isoclinal folding, southward nappe emplacement and syntectonic greenschist facies metamorphism. Deformation resulted from early Carboniferous (post Tournaisian) N-S crustal shortening and late Carboniferous extension (Carmignani *et al.*, 1994, 2001). The nappe stack is widely exposed across the main tectonic structure represented by the NW-SE trending Flumendosa Antiform (Carmignani *et al.*, 1994). Deformation and metamorphic grade show a remarkable increase across the Nappe Zone from the External Nappes at south towards the Internal Nappes at north. The highest intensity of deformation is reached in the internal nappes (Meana Sardo and Barbagia Units), characterized by widespread mylonitic deformation developed under greenschist facies conditions coeval with southward thrusting onto external units (Conti *et al.*, 1998). Within the external nappes the deformation and the metamorphic grade increase downward throughout the nappe stack from the uppermost Sarrabus and Gerrei Units to the lowermost Riu Gruppa and Monte Grighini Units (Caro-

si *et al.*, 1990; Conti *et al.*, 1998). Amphibolite facies conditions are reached in the Monte Grighini Unit in the core of the Flumendosa antiform (Musumeci, 1992; Cruciani *et al.*, 2016). Crustal thickening led to nappe emplacement followed by the development of km-scale upright WNW-ESE trending antiform and synform that refolded previous foliation and thrusts. This evolution corresponds to the  $D_1$  phase in the Sarrabus and Gerrei Units and to  $D_1$  and  $D_2$  phases in the Rio Gruppa and Monte Grighini Units (Carmignani *et al.*, 1994; Carosi *et al.*, 1990; Conti *et al.*, 2001). The late orogenic evolution resulted in the exhumation of deep tectonic units and crustal extension, driven by low- to high- angle normal faults, mainly developed on the limbs of antiform, and km-scale, strike-slip faults. According to Conti *et al.* (2001) these deformation correspond to the  $D_2$  and  $D_3$  phases and the late stage of tectonic activity was closely followed or partly coeval with late Carboniferous (305-285Ma) widespread intrusive magmatism (Carmignani *et al.*, 1994).

### THE MONTE GRIGHINI COMPLEX: GEOLOGICAL OUTLINE

The Monte Grighini Complex (MGC; Fig. 3), exposed in the External Nappe Zone at the western termination of the Flumendosa antiform, consists of superposed Paleozoic tectonic units and late Variscan synkinematic granitic intrusions (Musumeci, 1992; Musumeci *et al.*, 2015). Due to the occurrence of amphibolite facies metamorphic rocks it was at first interpreted as a pre-Variscan metamorphic basement of Caledonian age (Carmignani *et al.*, 1982). By the mid-eighties, detailed field surveys joined with structural and petrological studies allowed reinterpretation of the Monte Grighini Complex as a metamorphic complex of Variscan age marked by the occurrence of: (i) the deepest unit of the Nappe Zone; (ii) a major late Variscan strike-slip shear zone (Elter *et al.*, 1990); (iii) synkinematic intrusions of metaluminous (diorite to monzogranite) and peraluminous (leucogranite) composition (Cherchi & Musumeci, 1987; Musumeci, 1992).

### Lithostratigraphic units

The Variscan basement in the MGC consists of three superposed tectonic units with lower greenschist to upper amphibolite facies metamorphism and late Carboniferous intrusive rocks. From top to bottom of the nappe pile they are: Gerrei Unit, Castello Medusa Unit and Monte Grighini Unit.

**Gerrei Unit** - This unit, cropping out in the western and southern sides of complex (Fig. 3), consists of Middle Ordovician to Siluro-Devonian very low met-

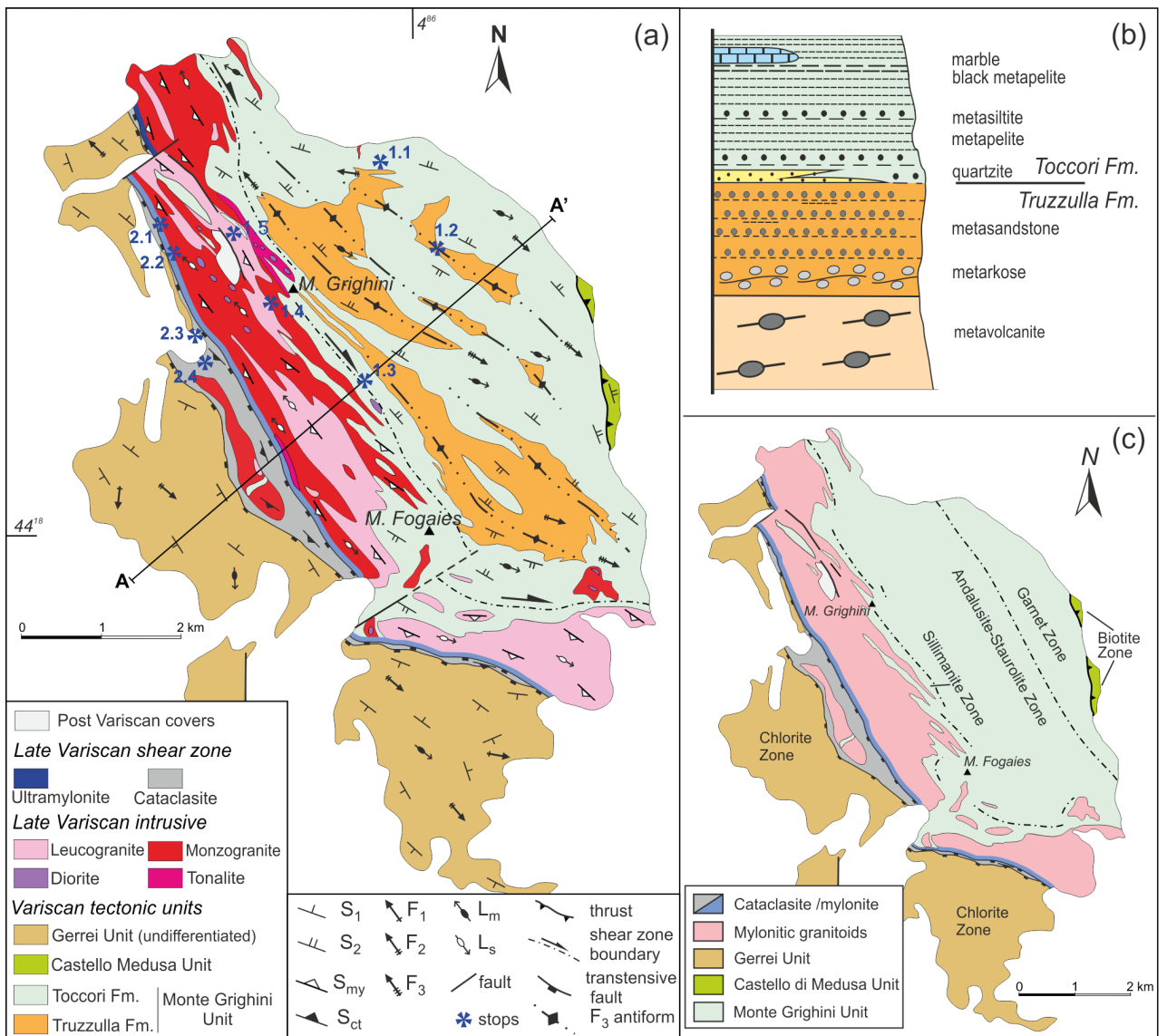


Fig. 3 - a) Geological sketch map of Monte Grighini Complex. Blue stars indicate the stops; b) lithostratigraphic column of Monte Grighini Unit; c) simplified map of metamorphic zonation. Modified after Cruciani *et al.* (2016) and references therein.

amorphous grade (lower epizone facies) metasediments and metavolcanics. The lithostratigraphic succession starts with Middle Ordovician metavolcanics (Carmignani *et al.*, 1994) of intermediate composition (Monte Santa Vittoria Fm.) upward followed by metasandstones and metarkoses (Su Muzziioni Fm.) and rhyolitic-rhyodacitic metavolcanics (Porfiroidi Fm.). The Upper Ordovician-Silurian succession starts with metarkoses and quartzites (Genna Mesa Fm.) followed by metapelites with fossiliferous metasilites (crynoid articles and inarticulated brachiopods) and thick fossiliferous (encrinite) metalimestones (Rio Canoni Fm.). Black shales with decameter-thick lenticular bodies of

nodular limestone correspond to the Siluro-Devonian succession (Scisti Neri Fm.).

**Castello Medusa Unit** - This unit crops out in a very limited extent at the easternmost side of the complex (Fig. 3). The lithostratigraphic succession comprises low metamorphic grade (upper epizone facies) metarkoses belonging to Upper Ordovician volcanoclastic (Genna Mesa Fm.), upward followed by metapelites with intercalated decameter-thick marble and calc-schist lenses belonging to the Sa Lilla Fm. of Upper Silurian-Devonian age.

**Monte Grighini Unit** - This unit crops out extensively in the northern and southern portion of complex

(Fig. 3) and consists of medium metamorphic grade (lower to upper amphibolite facies), lower Paleozoic metavolcanics (Truzzulla Fm.) and metasediments (Toccori Fm.) (Fig. 3b).

The Truzzulla Fm. consists of Upper Ordovician ( $447 \pm 4.3$  Ma) acidic metavolcanics, metarkoses and arkosic metasandstones of calc-alkaline affinity (Cruciani *et al.*, 2013b) followed upward by metarkoses and arkosic metasandstones with augen textures partitioned in intensely foliated domains.

The Toccori Fm. consists of metapelites with intercalated centimeter to decimeter-thick metasiltite layers (Cruciani *et al.*, 2013b) (now schist, micaschist and paragneiss) and hornfels schists mainly adjacent to, or enclosed as septa, in the granite. White quartzite levels mark the base of the Toccori Fm., whereas black graphitic metapelite and meter-thick marble lenses occur in the uppermost portion of the formation. According to Cruciani *et al.* (2016), the metamorphic grade increases toward west, from lower amphibolite facies (characterized by the presence of garnet, biotite, white mica, plagioclase) to upper amphibolites facies (characterized by occurrence of staurolite and/or andalusite in addition to garnet, biotite, white mica, plagioclase). The highest conditions are registered close to the contact with granitic intrusions with mineral assemblages of white mica, oligoclase, biotite, garnet, andalusite, sillimanite, K-feldspar and cordierite (Fig. 3c).

### Monte Grighini Intrusive Complex

The Monte Grighini Intrusive Complex is a NW-SE trending, subvertical sheet intrusion of Late Variscan age (305-295 Ma) emplaced in the Monte Grighini Unit (Fig. 3 and Fig. 4). On the basis of mineral assemblages and geochemical signatures, a diorite, tonalite, monzogranite suite (I-type calc-alkaline metaluminous suite) and a leucogranite one (S-type peralumi-

noussuite) have been defined (Del Moro *et al.*, 1991b). Both metamorphic and intrusive rocks are crosscut by ENE-WSW and NW-SE trending aplitic/pegmatitic dikes and quartz dykes (Musumeci *et al.*, 2015).

**Calc-alkaline suite** - This suite mainly consists of monzogranite with minor bodies of tonalities and diorite. Monzogranite forms a wide NW-SE elongated sheet intrusion exposed in the central and northern portion of the massif. This intrusion extends eastward at shallow depth and locally crops out in the northern and southern portions of the Monte Grighini Unit. These rocks give a K/Ar biotite age of  $305 \pm 6$  Ma (Musumeci, 1991a). Biotite-bearing, medium- to fine-grained tonalites occur in two NW-SE elongated small sheet bodies localized along both the eastern and western sides of monzogranite intrusion. An igneous foliation marked by plagioclase and biotite alignment characterizes the tonalite fabric. Fine-grained, biotite-bearing diorites occur as decameter-thick bodies within tonalite and as centimeter- to decimeter-thick enclaves within monzogranites. Diorite gives a K/Ar biotite age of  $302 \pm 6$  Ma and Rb/Sr biotite ages of  $294 \pm 9$  Ma and  $293 \pm 4$  Ma (Del Moro *et al.*, 1991b).

**Peraluminous suite** - Fine-grained, muscovite-bearing leucogranite forms a wide NW-SE elongated sheet intrusion extending from the northwestern to the southeastern side of the Monte Grighini Complex. Mineral assemblages are (i) quartz + K-feldspar + plagioclase + K-white mica + biotite + garnet and (ii) quartz + K-feldspar + plagioclase + K-white mica + garnet + biotite. The muscovite-bearing assemblage dominates in the southern portion (Su Cruccuri) while K-white mica- and biotite-bearing assemblages occur in the northern portion (Cuccuru Mannu). Rb/Sr in muscovite determination gives an age of  $305 \pm 6$  Ma in a meter-thick undeformed dyke and average age of  $298 \pm 2$  Ma for large-scale leucogranite bodies that well match the Ar/Ar muscovite age of  $302 \pm 0.24$  Ma (Del Moro *et al.*, 1991b).

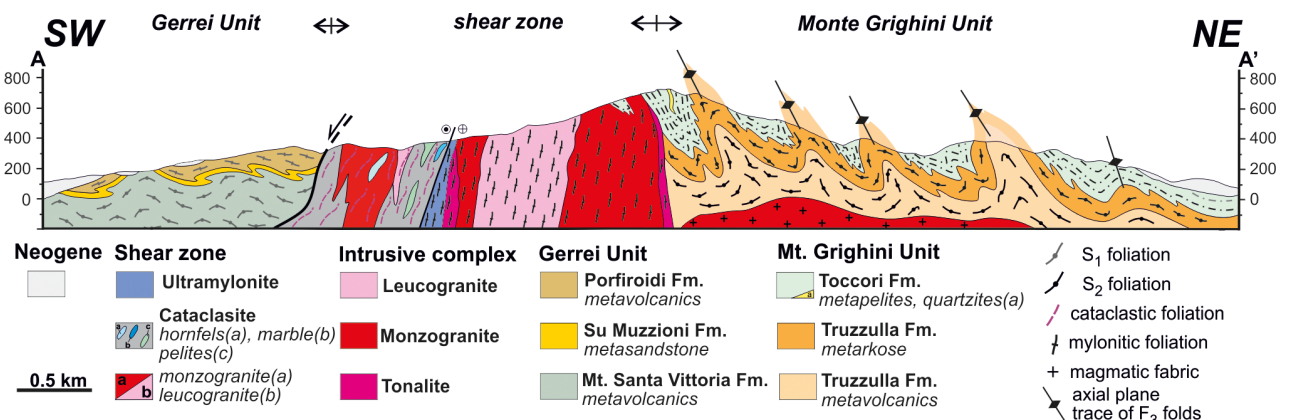


Fig. 4 - Geological cross section of the Monte Grighini Complex along the line A-A' in Fig. 3 (from Cruciani *et al.*, 2016).

## TECTONIC AND METAMORPHIC FEATURES

The tectonic units experienced a polyphase Variscan tectonic and metamorphic evolution characterized by syn-collisional shortening deformation related to the regional-scale southward nappe stacking ( $D_1$  and  $D_2$  phases of nappe zone; Carmignani *et al.*, 1994; Conti *et al.*, 2001) followed by late Variscan extensional and transtensive tectonics (Carmignani *et al.*, 1994; Musumeci, 1992). The resulting structural framework is well shown in the geological section of Fig. 4 (from Cruciani *et al.*, 2016).

**Syn collisional structure**

The early shortening and nappe stacking deformation results in the development of southwestern verging folds with NW-SE striking axial plane foliations representing the main planar fabric at meso and macroscopic scale. This shortening deformation corresponds to the  $D_1$  phase in the Gerrei Unit and  $D_1$  -  $D_2$  phases in the Castello Medusa and Monte Grighini Units, with NW- to WNW-trending isoclinal folds overturned towards the south-southwest and NW striking axial plane foliation ( $F_1$  -  $S_1$  Gerrei Unit and  $F_2$  -  $S_2$  Castello Medusa and Monte Grighini Unit). In this latter unit the first  $S_1$  schistosity is preserved as relict foliation recognizable in correspondence of tight to isoclinal intrafoliar folds verging toward southwest. The relationships between deformation, folding phases, and metamorphic grade in the tectonic units belonging to the Monte Grighini Complex are shown in Table 1. The early shortening deformation ( $D_1$  and  $D_2$  phases) developed under lower greenschist facies in the Gerrei

Unit while Castello Medusa and Monte Grighini units experienced syn- $D_2$  metamorphism under greenschist facies and amphibolite facies conditions, respectively. In the Monte Grighini Unit amphibolite facies conditions are testified by syn- $D_2$  growth of garnet and staurolite assemblages and syn-post- $D_2$  growth of andalusite, sillimanite/fibrolite and cordierite assemblages; these latter appear in the metasediments hosting the magmatic bodies belonging to the Intrusive Complex. According to Cruciani *et al.* (2016), the metasediments of Monte Grighini Unit reached pressure conditions of 0.7-0.9 GPa with temperatures ranging between 475-540°C (baric peak) at the beginning of the  $D_2$  phase. Baric peak was followed by decompression with attainment of P-T conditions of 0.35-0.55 GPa and 520-580°C at the end of the  $D_2$  phase, coeval with the emplacement of metaluminous and peraluminous granitic intrusions.

**Late collisional structure**

Early structures were deformed by successive deformation phases ( $D_2$  phase Gerrei Unit,  $D_3$  phase Castello Medusa Unit and  $D_3$ - $D_4$  phase in the Monte Grighini Unit; Conti *et al.*, 2001; Musumeci *et al.*, 2015). Late folding structures are represented by large scale NW-SE trending upright antiform and synform ( $F_2$  fold Gerrei Unit and  $F_3$  fold Castello Medusa Unit and Monte Grighini Unit; Fig. 4). The  $F_3$  folds in Castello Medusa and Monte Grighini Units are characterized by axial plane crenulation cleavage with synkinematic recrystallization of white mica, chlorite and Fe-oxides. The  $D_4$  phase localized in the Monte Grighini Unit and in the easternmost side of Gerrei Unit corresponds

Table 1 - Deformation phases and related metamorphic events in the different tectonic units of Monte Grighini Complex. L-MG: low metamorphic grade; M-MG: medium metamorphic grade. From Musumeci *et al.* (2015).

	Variscan nappe stacking		late Variscan deformation	
<b>Monte Grighini Unit</b>	<b>D<sub>1</sub> phase</b> fold $F_1$ fold - $S_1$ foliation L-MG (Wmca + Chl ± Bt)	<b>D<sub>2</sub> phase</b> fold and thrust $F_2$ fold - $S_2$ foliation (Wmca + Bt ± Grt ± St) Post- $S_2$ (And ± Sil ± Crd)	<b>D<sub>3</sub> phase</b> late fold $F_3$ fold - $S_3$ foliation	<b>D<sub>4</sub> phase</b> strike-slip shear zone shear band - mylonites brittle fault - cataclases (Wmca + Qtz)
<b>Castello Medusa Unit</b>	<b>D<sub>1</sub> phase</b> fold $F_1$ fold - $S_1$ foliation L-MG (Wmca + Chl)	<b>D<sub>2</sub> phase</b> fold and thrust $F_2$ fold - $S_2$ foliation L-MG (Wmca + Chl ± Bt)	<b>D<sub>3</sub> phase</b> late fold $F_3$ fold - $S_3$ foliation	
<b>Gerrei Unit</b>	<b>D<sub>1</sub> phase</b> fold and thrust $F_1$ fold - $S_1$ foliation L-MG		<b>D<sub>2</sub> phase</b> late folding $F_2$ fold	<b>D<sub>3</sub> phase</b> strike-slip shear zone brittle faults cataclases

to a kilometer-wide NW-SE trending dextral strike-slip shear zone with shear displacement of at least 6-7 kilometers (Musumeci, 1991b) and is marked by the synkinematic emplacement of the Intrusive Complex (Fig. 3 and Fig. 4). This late collisional structure is the main tectonic lineament of the Monte Grighini Complex and one of the main late Variscan strike-slip shear zones in Sardinian Variscan chain (Elter *et al.*, 1990; Musumeci, 1992). Shear deformation overprinted all previous foliations ( $S_1 - S_3$ ) and metamorphic assemblages of Monte Grighini Unit metasediments, and developed under retrograde conditions from amphibolites to lower greenschist facies, this latter testified by extensive growth of fine-grained white mica as a product of retrograde alteration of previous metamorphic and igneous mineral assemblages. Shear deformation is characterized by an increasing gradient from NE to SW, which define a succession of NW-SE trending deformation zones from protomylonite to the east to ultramylonite to the west. This latter corresponds to a decameter-thick continuous belt marking the western side of the shear zone (Fig. 3 and Fig. 4). At mesoscopic scale, shear fabrics are NW-SE trending C-type shear bands and mylonite-ultramylonite foliations that steeply dip toward the southwest ( $70-80^\circ$ ) and bear subhorizontal to gently plunging ( $10-25^\circ$  toward NW) mineral lineations. The C-type shear bands occur throughout the shear zone from protomylonite to mylonite zone and correspond to the main foliation in the ultramylonite zone where the largest shear strains are reached (Musumeci, 1991b). Along the westernmost and the southernmost portions of the shear zone NW-trending detachment fault marks the tectonic contact with the Gerrei Unit. Detachment fault consists of a westward dipping cataclastic zone of variable thickness (decimeter to hectometer), made up of highly brecciated and cataclastic metamorphic and igneous rocks (Fig. 3 and Fig. 4). Southwest dipping cataclastic foliations and brittle shear planes, overprinting all previous foliations and/or fabric, show a top-to-the-southwest sense of shear movement. Detachment fault and cataclastic zone are related to the brittle deformation that characterizes the late stage of the shear zone activity (Musumeci, 1992).

Ductile to brittle shear deformation affected the whole late Carboniferous Intrusive Complex (peraluminous leucogranites and calc-alkaline tonalite-monzogranites). On the basis of (i) the NW-elongated shape of intrusions parallel to the shear zone, (ii) the transition from WNW-striking magmatic foliation to NW-striking steeply dipping shear bands, and (iii) shear deformation of synkinematic porphyroblasts (andalusite) in the high metamorphic grade host rocks, the emplacement of the Intrusive Complex as a whole is regarded as synkinematic to the shear zone. Thus, on the basis of available ages of synkinematic intrusions (Carmi-

gnani *et al.*, 1987; Del Moro *et al.*, 1991b; Laurenzi *et al.*, 1991) the shear zone activity ranges from 305 to 295 Ma (Elter *et al.*, 1990; Musumeci, 1992).

#### DISCUSSION: TECTONIC AND METAMORPHIC HISTORY

The Monte Grighini complex is an outstanding example of nappe stack where tectonic units that experienced syn to late-collisional evolution at different crustal levels are well exposed. In particular, is the unique tectonic complex of External Nappe Zone where the deepest levels of nappe stack and synkinematic intrusion can be examined. Thus, these features allow to investigate the relationship between tectonic, metamorphic and magmatic processes in a deep section of the Variscan crust farther south of the Axial Zone.

The P-T path reconstructed for the Monte Grighini Unit metasediments indicates a clockwise loop (Fig. 5), corresponding to an orogenic evolution with an initial burial, followed by heating during decompression and exhumation (Cruciani *et al.*, 2016). The baric peak (0.7-0.9 GPa, 475-540°C) points to an underthrusting with deep burial to about 30 km depth (Cruciani *et al.*, 2016). The peak conditions of burial event postdated the  $D_1$  deformation, being pre-syn the early stage of the  $D_2$ . This implies that the deep burial recorded by this unit was reached during the underthrusting of Palaeozoic sequences of External Nappes ( $D_1$  and  $D_2$  phase). Thus, in this unit crustal shortening and nappe stack is recorded by the  $S_1/S_2$  foliations and  $F_2$  folds. Differently, at upper crustal level (i.e. Gerrei Unit) shortening and nappe stacking was recorded by  $S_1$  foliation and  $F_1$  folds. Decompression and first exhumation of the Monte Grighini Unit to higher crustal levels (18-15 km) was accompanied by heating ( $T = 520-580^\circ\text{C}$ ,  $P = 0.35-0.55$  GPa) and the almost coeval intrusion of metaluminous and peraluminous granitic melts. Indeed, the P-T conditions of granite bodies indicate depths of emplacement of about 18 km, which is similar to the depth estimated for the peak metamorphism in the metasediments of Toccori Fm. at the end of the  $D_2$  deformation. Therefore, thermal peak conditions, recorded by sillimanite-bearing assemblages in metasediments of Toccori Fm. mainly reflect a large scale perturbed thermal state of the crust as also evidenced by generation of peraluminous melts. This means that the deepest level of the nappe stack experienced partial melting (anatexis) as a consequence of high geothermal gradient during the late orogenic stage in this portion of the Variscan belt.

The final exhumation of deep Monte Grighini Unit to upper crustal level occurred under retrograde (pressure and temperature) metamorphic conditions and was associated with upright folding ( $D_3$  phase) and

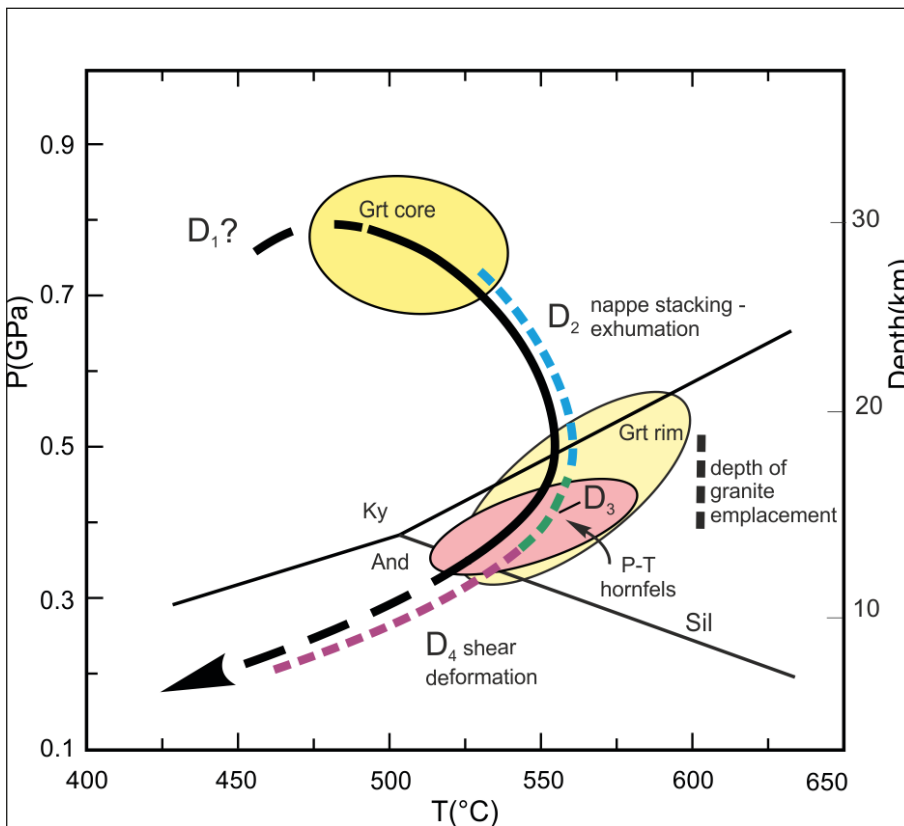


Fig. 5 - P-T path for the Monte Grighini rocks. Ellipses' size refer to the estimated errors. The yellow ellipses represent P-T conditions inferred from the garnet core and rim and white mica compositions of micaschists from the Toccori Fm. The pink ellipsis represents P-T conditions estimated for the hornfelsed schist. Vertical dashed line represents estimated depth of granite emplacement. Colored dashed line roughly represents the relationships between P-T and deformation events. From Cruciani *et al.*, 2016.

ductile to brittle activity of shear zone and detachment faults ( $D_4$  phase). Upright open folds with large wavelength also affected the overlying tectonic units ( $F_3$  folds in the Castello Medusa Unit and  $F_2$  folds in the Gerrei Unit). Ductile shear zone acted as a preferential pathway for magma rise and emplacement, and the activity of both shear zone and detachment fault produced the final setting leading to the contact between the deepest and the uppermost tectonic units of External Nappe Zone.

Available radiometric data (Rb/Sr and Ar/Ar cooling ages on metamorphic and magmatic mica; Carmignani *et al.*, 1987; Del Moro *et al.*, 1991b) consistently suggest that (i) emplacement of metaluminous and peraluminous intrusions, (ii)  $D_3$  folding and  $D_4$  dextral strike-slip shear zone and detachment fault likely occurred in a narrow time span (305-295 Ma) in the late Carboniferous-early Permian. Moreover, the similar ages of peraluminous intrusions and thermal peak in the host metamorphic rocks allow us to delineate the occurrence of crustal anatexis with S-type melts coeval with metamorphism in the lower-middle crust in the External Nappe Zone.

The reconstructed P-T-t path for the Monte Grighini Unit contributes to a better understanding of the tectonic evolution of the Nappe Zone and the rela-

tionships with the Axial Zone of the Variscan belt in northern Sardinia. In particular, the baric condition-recorded by this unit means that the deep portion of the external unit nappe stack underwent to deep underthrusting in the accretionary wedge during the early collisional phase. Other units (i.e. Gerrei Unit and Sarrabus Unit) experienced moderate to lower underthrusting representing the upper portions of the accretionary wedge. Moreover, geological data issuing from Monte Grighini Complex allow to depict the diachronicity of the metamorphic-tectonic evolution across the collisional belt from the Axial to the External Nappe Zone. Indeed, the main tectonic and metamorphic events related to the building of the chain (i.e. syn to late collisional) show a difference in age of about 10-20 Ma (Cruciani *et al.*, 2016).

In particular, a relevant feature is the diachronicity of thermal perturbation leading to crustal anatexis and LP/HT metamorphism, the ages of which ranges between 330-320 Ma in the migmatitic complex of the Axial Zone (Schneider *et al.*, 2014; and references therein) to 305-295 Ma in the External Nappe (Cruciani *et al.*, 2016). Hence, the external units experienced a metamorphic evolution (burial, exhumation and thermal heating) strictly similar to that recorded by the inner units with a significant diachronicity of

tectono-metamorphic events. Thus, the ductile shear zone that is the most relevant tectonic lineament of Monte Grighini Complex is likely the most external and youngest (305-295 Ma) strike-slip shear zone in the Variscan belt of Sardinia, that contribute to final exhumation and played a major role in the drainage of synkinematic melts from deep partially molten crust in late Variscan time.

#### FIELD GUIDE TO THE EXCURSION

Monte Grighini (Figs. 6, 7) is a Regional Forestry complex of about 5000 ha, belonging to several surrounding villages. It is supervised by "Fo.Re.S.T.A.S." regional agency, that also attends to the in progress reforestation.

To reach Monte Grighini from Cagliari take the highway S.S. 131 northward until the exit to Simaxis (km 93). After crossing the village, take the S.P. 35 toward

Siamanna and follow driving directions to Allai (on the left at the roundabout before Siamanna, S.P. 39). After about 8 km, turn on the right to enter in the main paved road of the Monte Grighini Complex through an iron gate.

From Olbia take the S.S. 131dcn toward Abbasanta and then take the S.S. 131 southward until the exit to Simaxis. The stops localization is shown in Figs. 6, 7.

#### First Day

##### **Stop 1.1 - Toccori Formation - garnet+staurolite-bearing micaschist (Coord. 8°49'48.41"E - 39°57'19.59"N)**

The first stop is located along the main paved road that crosses the Monte Grighini Complex, at the third hair-pin turn (about 1 km from the entrance gate) where a lateral pathway insert in it. From here, looking to the east we can see the Allai plain.

The outcrop consists of a garnet + staurolite micaschists (Fig. 7) belonging to the Toccori Fm. (Monte

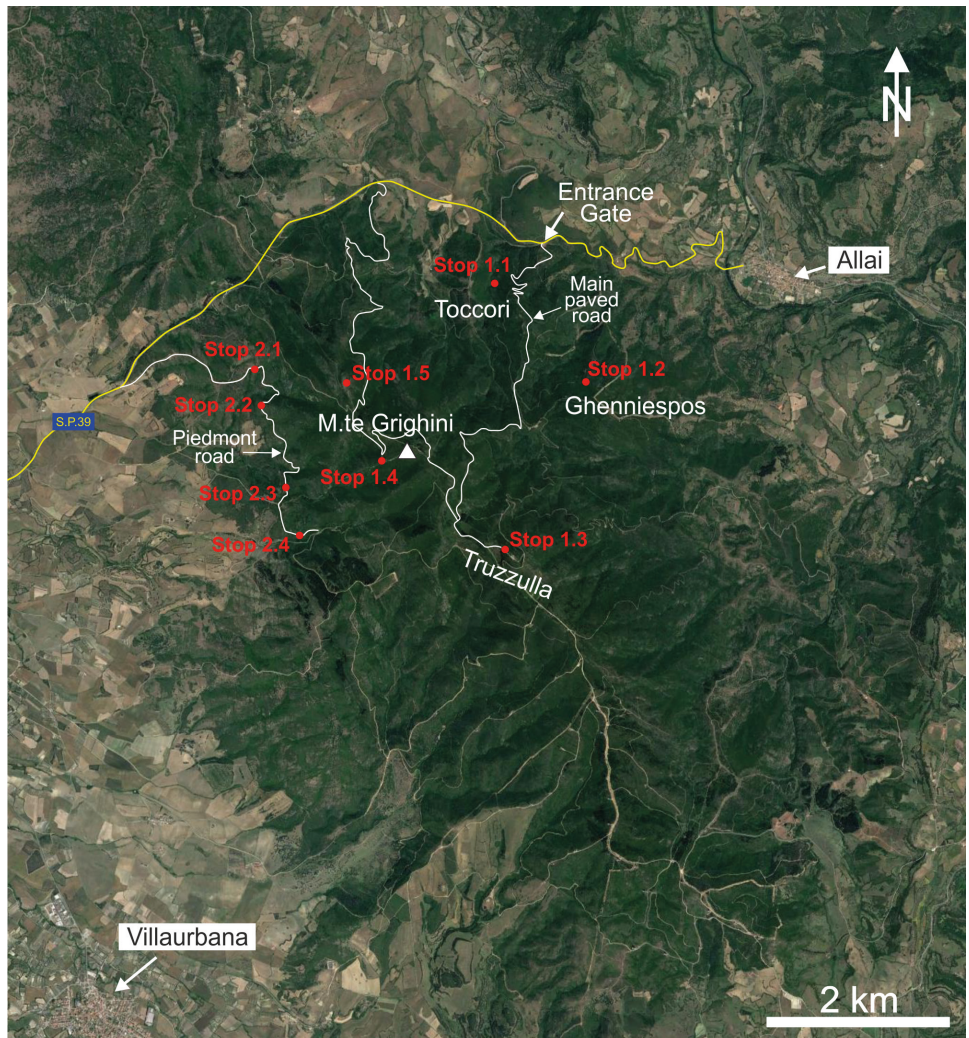


Fig. 6 - Satellite image of Monte Grighini Complex with the position of field stops. (Image from Google Earth);

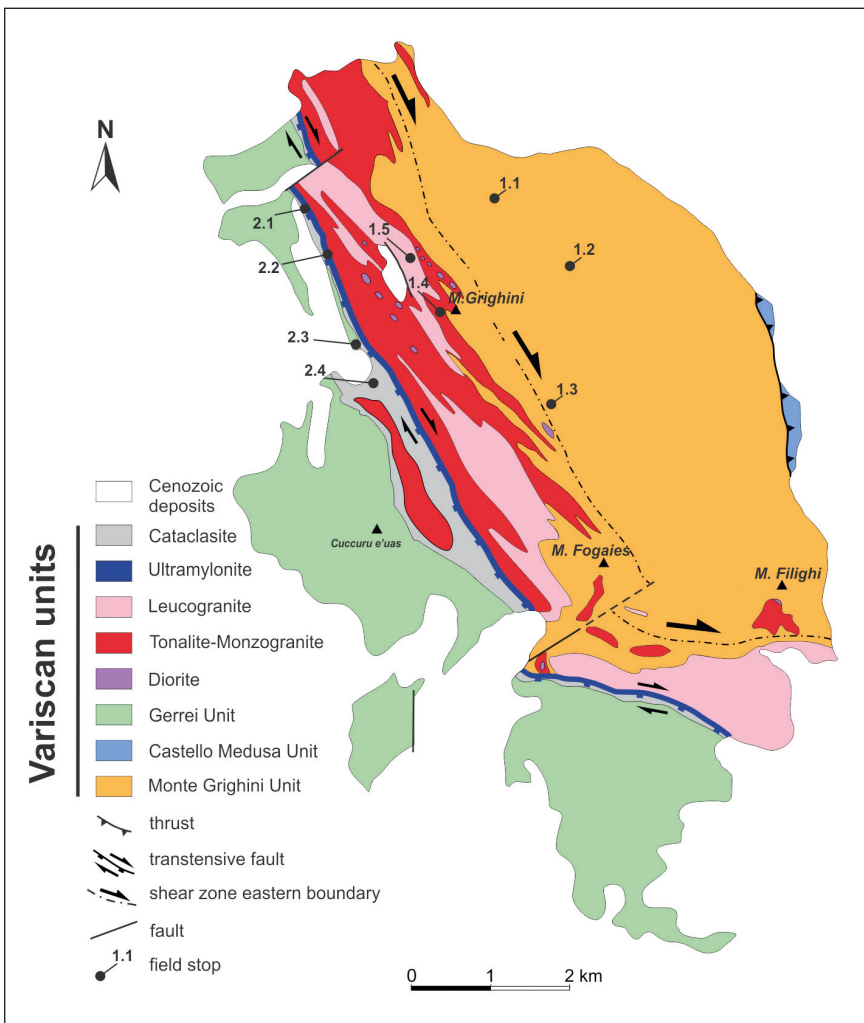


Fig. 7 - Tectonic sketch map with the position of stops (modified from Musumeci *et al.*, 2015).

Grighini Unit) well exposed along the road cut. According to Musumeci *et al.* (2015) and Cruciani *et al.* (2016), Toccoi Fm. represents the upper part of the volcanic-sedimentary Monte Grighini Unit, whereas the base is represented by Truzzulla Fm.

Micaschists of Toccoi Fm. are dark, fine- to medium-grained, well-foliated rocks, sometimes alternating with metarkoses. At the naked eye is possible to distinguish rounded, submillimeter-sized plagioclase, garnet and biotite. Structural framework is characterized by a pervasive  $S_2$  foliation that strikes  $N80-110^\circ$  and moderately dips ( $55-60^\circ$ ) to NNE or SSW.  $D_3$  phase is expressed by  $N90-100^\circ$ -trending open folds with subhorizontal axes and  $N95-100^\circ$  striking axial planes, with a well developed  $S_3$  crenulation cleavage (Fig. 8a-b). Relics of a previous metamorphic foliation ( $S_1$ ) are recognizable in correspondence of centimeter-sized, isoclinal, intrafoliar folds (Fig. 8a). The protolith of garnet + staurolite metasediments was a pelitic-psammitic sequence, as

shown by the micaschists/metarkoses alternations, that underwent a greenschists to amphibolite facies metamorphism.

In the micaschists several decimeter-sized, fine-grained, foliated, quartz-feldspathic layers are commonly found (Fig. 8c). They represent WNW striking foliated aplite dykes parallel to schistosity ( $S_2$ ) of host micaschist. In other parts of the complex, aplite dykes are discordant and not foliated (see Stop 1.2). Going uphill along the road cut, alternation of paragneiss and metavolcanics levels appears, marking the transition from the Toccoi Fm. to the Truzzulla Fm.

In thin section micaschists appear as medium- to fine-grained rocks that are made up of  $Grt + Bt + Wmca + Pl + Qtz \pm St \pm And \pm Chl$  (abbreviations according to Fettes & Desmons, 2007); accessory phases are K-feldspar, apatite, ilmenite, zircon, monazite, epidote and Fe-oxides. The fine-grained matrix consists of alternating quartz-feldspathic and phyllosilicate

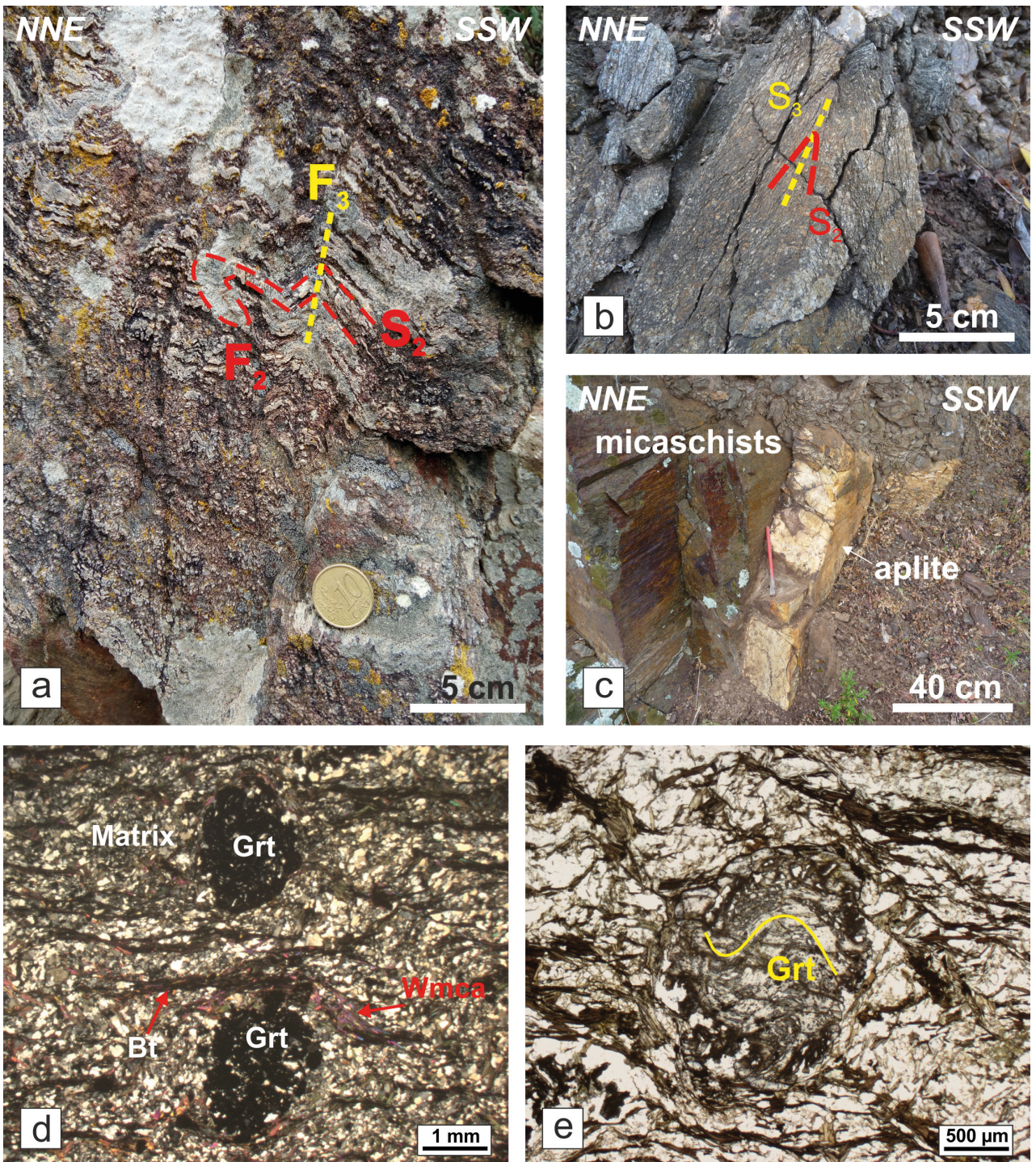


Fig. 8 - a) Structural framework of Grt+St-bearing micaschists with  $F_2$  intrafoliar fold,  $S_2$  main foliation and late  $F_3$  folds; b)  $F_3$  folds and  $S_3$  crenulation cleavage in micaschists; c) foliated aplite dyke hosted in micaschists; d) microphotograph of the texture of garnet-bearing micaschists with subhedral garnets immersed in a quartz-feldspathic matrix with oriented phyllosilicates trails; e) detail of garnet with rotational structures.

rich layers, hosting garnet and plagioclase porphyroclasts (Fig. 8d). Garnet shows anhedral to subhedral habitus, is compositionally zoned and sometimes exhibits rotational microstructure (Fig. 8e). Common inclusions in garnet are quartz, plagioclase, white mica and accessory phases (zircon, monazite, titanite and Fe and Ti oxides). Phyllosilicate-rich matrix is strongly oriented according to the  $S_2$  and hosts submillimeter-sized staurolite. Cordierite has not been found in this area but occurs as submillimeter-sized, altered crystals in the southern portions of the Monte Grighini Unit.

From Stop 1.1 we drive along the same paved road for few hundreds of meters and then we take on the left a dirt road southwestward. We drive for less than one kilometer and then park in a small area at the base of the Ghenniespos hill, at a few hundreds of meters from the metavolcanic outcrop.

### Stop 1.2 - Truzzulla Formation metavolcanics (8°50'23.13"E - 39°56'48.44"N)

At Ghenniespos locality (Figs. 6, 7) the basal part of Truzzulla Fm. and thus of the whole Monte Grighini Unit can be observed. This outcrop consists of two subparallel, decameter-sized bodies of metavolcanic rocks belonging to the Truzzulla Fm. (Fig. 9a) that form the core of a large E-W oriented antiform (Ghenniespos antiform) in the northeastern part of the Monte Grighini Complex. The metavolcanics are surrounded by the metarkose and arkosic metasandstones of the Truzzulla Fm. that in turn are overlain by the metapelites of the Toccori Fm. The field relationships with the metapelites of the Toccori Fm. point out that the latter represent the sedimentary cover of the volcanic-volcanoclastic sequence of Truzzulla Fm. (Cruciani *et al.*, 2013b).

The metavolcanics are characterized by a well-devel-

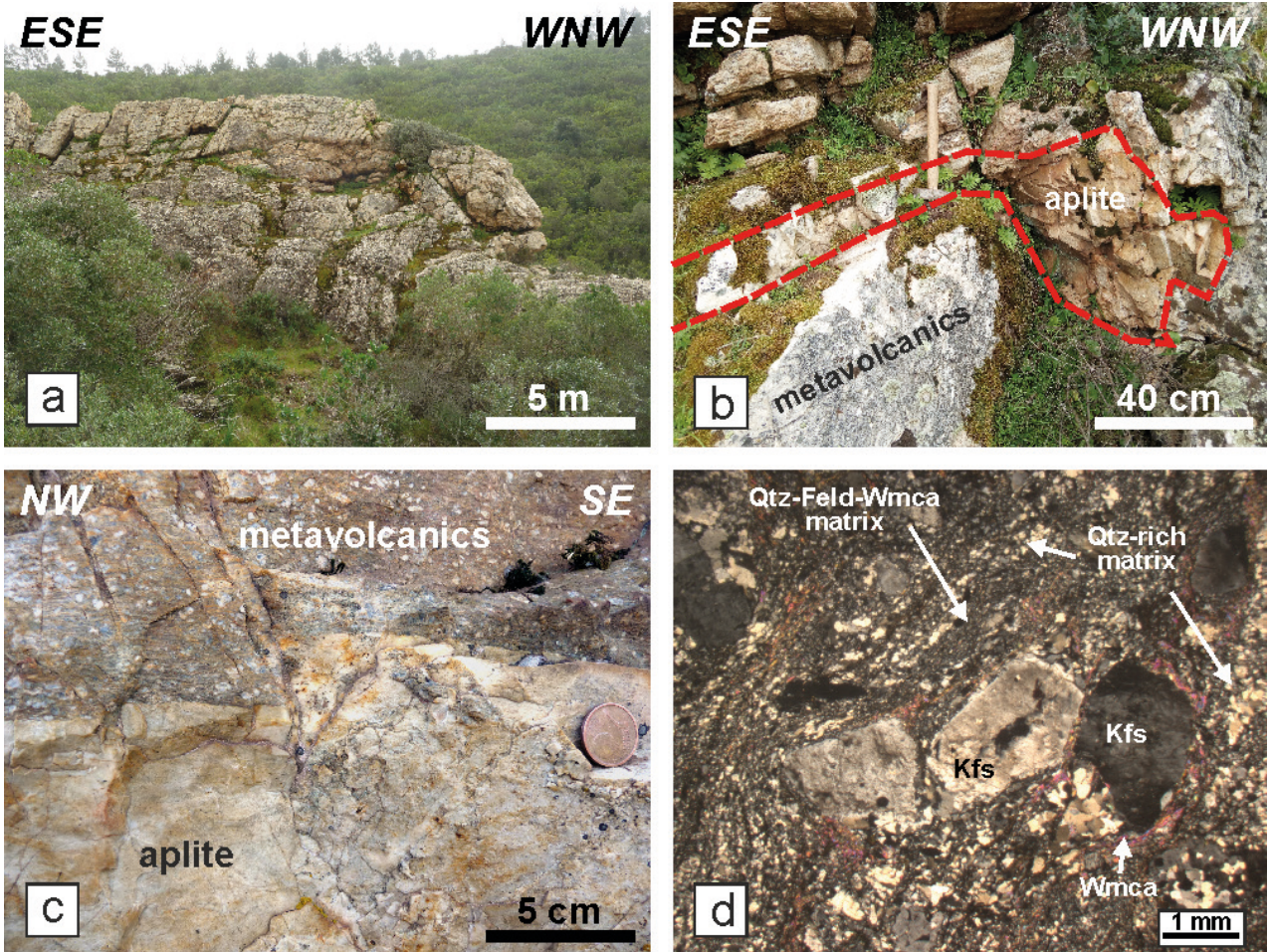


Fig. 9 - a) View from north of the southern metavolcanic body; b) aplite dyke hosted in metavolcanics. On the left side of the photo the dyke is subparallel to the main foliation; c) close up view of the sharp contact between metavolcanics and aplite dyke; d) Photomicrograph of metavolcanics from Ghenniespos. Note the alternation between coarse grained Qtz-rich levels and finer-grained Qtz-Feld-Wmca-rich ones (1.25X - crossed polars).

oped E-W trending  $S_2$  foliation with a large amount of rounded to subrounded quartz and feldspar porphyroclasts visible at the naked eye.

In the southern body, the hinge zone and southern limb of the large antiform crop out. Here, in the limb zone, the  $S_2$  foliation strikes N100° and moderately dips toward south, whereas in the hinge zone the  $S_2$  foliation becomes subhorizontal. On this foliation surface, a quartz mineralogical lineation strikes N100° and dips 10° to the E.

Within the metavolcanics a fine-grained, light-colored, aplitic dyke crosscuts the foliation of the hosting metavolcanics. On its eastern side, the dyke progressively thins and its strike becomes subparallel to the foliation of the metavolcanics (Fig. 9b, c).

At the thin section scale the Truzzulla Fm. metavolcanics show a weakly developed augen texture (Fig. 9d) consisting of Qtz + Kfs + Ab + Bt + Wmca, with accessory zircon, monazite, apatite and Fe-oxides. The porphyroclasts/matrix ratio has been visually estimated at ~30/70. K-feldspar, plagioclase (now albite) and quartz are thought to be of igneous origin. Microcline occurs as subhedral crystals up to ca. 3-4 mm in size surrounded by oriented phyllosilicates and partially replaced by recrystallized quartz. K-feldspar, plagioclase and quartz are stretched and deformed following the  $S_2$  foliation. The matrix is mainly made up of quartz, albite, K-feldspar and  $S_2$ -oriented biotite and K-white mica, locally arranged in alternating coarser- and finer-grained levels; the former are quartz rich, the latter

are quartz-feldspathic with variable amount of micas (Fig. 9d).

A metavolcanic sample collected from one of these two lenses yielded a zircon weighted average  $^{206}\text{Pb}/^{238}\text{U}$  protolith age of  $448 \pm 5$  Ma (Cruciani *et al.*, 2013b). According to these authors, the volcanic and volcanoclastic rocks of the Truzzulla Formation have a Katian age (Late Ordovician) since all the analyzed samples give a relatively well-defined age close to 447 Ma. The scatter toward slightly younger ages (about 430 Ma, Early Silurian) characterizing the samples of the Truzzulla Fm. can be explained with a lead loss that most likely occurred during the LP/HT contact metamorphism related to the intrusion of Late Carboniferous intrusive rocks in the Monte Grighini Unit.

From Ghenniespos we come back to the paved road and then we go uphill until we reach the fire lookout tower. Along this road we are crossing the Toccori Fm.

### Stop 1.3 - Truzzulla-Fire lookout tower (8°49'50.83"E - 39°55'47.19"N)

In this area (Figs. 6, 7) both Toccori Fm. and Truzzulla Fm. crop out. The former consists of micaschists with decameter thick quartzitic lenses (50-60 m in width and more than 1 km in length). The Truzzulla Fm. consists in NW-SE-elongated metasandstones and metarkoses bodies, that in the landscape form well recognizable rocky outcrops. The structural setting of this area and the relation between the different formations are schematized in the geological cross section of Fig. 10.

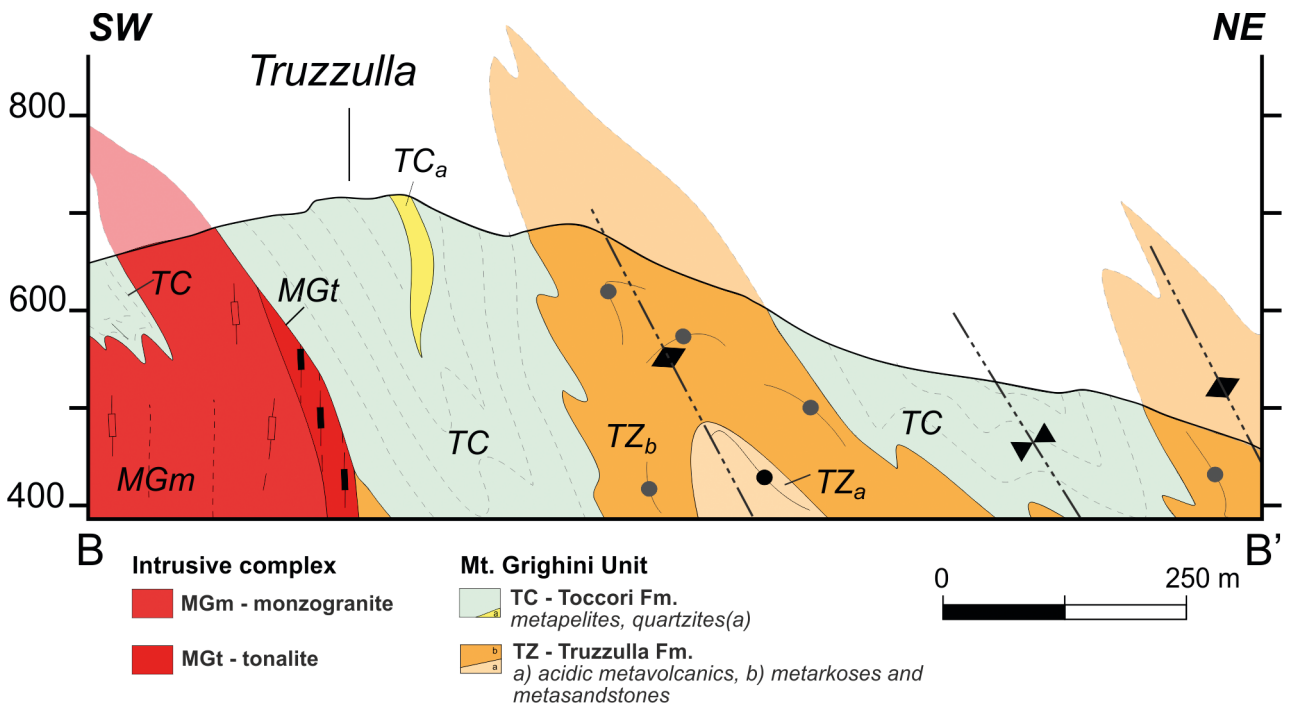


Fig. 10 - Detail of the geological cross section of Fig. 4 around Truzzulla (from Musumeci *et al.*, 2015, modified).

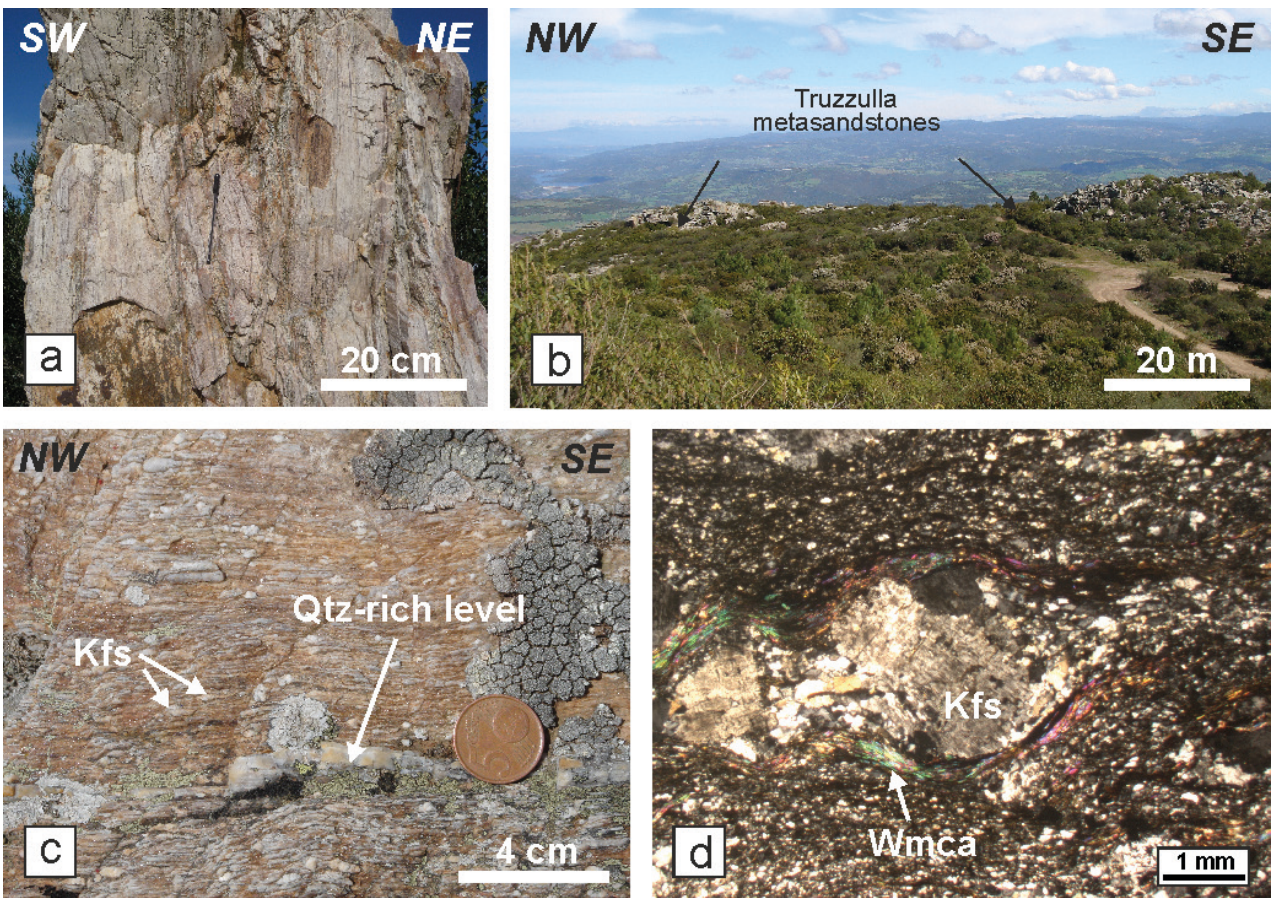


Fig. 11 - a) Field photograph of foliated, mica-rich quartzite from Truzzulla; b) panoramic view of metasandstones/metarkoses Truzzulla outcrop, from the fire lookout tower; c) detail of metasandstone texture, with deformed K-feldspar porphyroclasts and quartz-rich layers, elongated according to the main foliation; d) photomicrograph of metasandstone with a large K-feldspar surrounded by fine grained matrix and elongated micas; on its right side there is a Qtz+Wmca pressure shadow.

Quartzite lenses, that mark the contact between the top of Truzzulla Fm. and the base of the Toccori Fm., are light grey-pinkish, fine-grained, well-foliated rocks, formed by alternating quartz-rich and quartz+micas-rich layers (Fig. 11a). The here used term “quartzite” includes quartzite *s.s.* (>80% vol. of quartz), mica-rich quartzite and quartz-rich metasiltite. Structural framework is dominated by a NW-SE trending pervasive foliation ( $S_2$ ), steeply to moderately dipping toward NE. At the thin section scale  $S_2$  foliation is marked by millimeter-sized, quartz-rich layers alternating with thin mica-rich layers. Quartzite paragenesis is formed by Qtz + Wmca  $\pm$  Bt  $\pm$  Kfs  $\pm$  Chl; accessory phases are tourmaline and oxides. Quartz occurs in equigranular domains showing evidence of dynamic recrystallization with involvement of sub-grain rotation (SGR) and grain boundary reduction area (GBAR) processes. White mica forms submillimeter-sized, strongly oriented crystals, commonly concentrated in thin layers.

In this area the Toccori Fm. consists of garnet-staurolite-bearing and staurolite-andalusite-bearing mica-schists. The main  $S_2$  foliation is crosscut by mylonitic shear bands highlighted by centimeter-spaced NW-SE striking shear planes. These outcrop-scale shear structures mark the eastern boundary of the strike-slip shear zone and the beginning of mylonitic deformation (protomylonite zone; Musumeci *et al.*, 2015). From here, moving westward the mylonitic deformation increases reaching the highest degree in the ultramylonite zone. In thin section quartz is commonly recrystallized and biotite and muscovite are strongly oriented marking the foliation. From the tower, following the dirt road northeastward for 200 m, we intercept two metarkoses bodies outcropping on both sides of a lateral pathway (Fig. 11b). The left outcrop (coord.  $8^{\circ}49'54.27''E$  -  $39^{\circ}55'51.15''N$ ) offers the best rock exposition as well as the best overview of the northeastern side of the complex. Metarkoses from Truzzulla (Type Locali-

ty of these rocks) have augen texture with millimeter-sized K-feldspar porphyroclasts and quartz-rich levels surrounded by thin phyllosilicate-rich layers (Fig. 11c). Locally it is possible to observe a reduction in the porphyroclasts content and an enrichment in micas suggesting a heterogeneity of the sedimentary protolith (metasandstones). Thin section observation shows feldspar-rich levels alternating with quartz and quartz+mica-rich levels defining the  $S_2$  schistosity. K-feldspar porphyroclasts, ranging in size from 1 to 2-3 mm, are strongly deformed and commonly show pressure shadows formed by microcrystalline white mica and quartz (Fig. 11d). Plagioclase usually forms anhedral to subhedral, small crystals (~0.5 mm) in the matrix but is also found as inclusion in K-feldspar.  $^{206}\text{Pb}/^{238}\text{U}$  zircon dating on metarkoses sample yield an age of  $447\pm 6$  Ma, quite close to the age of metavolcanics of Ghenniespos (Cruciani *et al.*, 2013b).

From this point we have a good overview of the geology of the Monte Grighini Complex. Looking toward NW we can see three subparallel, elongated metarkoses lenses that represent  $D_3$  antiform structures. In the same direction we can see the top of Monte Grighini (670 m a.s.l.) with its characteristic quartz dyke on the southern slope. Looking toward NE there is the Lachixeddus valley; the wide, brownish, rocky outcrop at the valley bottom is made up by metavolcanics similar to those of Ghenniespos. These latter cannot be seen from here because are located on the opposite slope of the northern crest.

From Stop 1.3 we continue towards NW along the dirt road for approximately 2 km until we reach two hairpin bends, at a short distance one from the other; we park at the second bend on the left side of the dirt road and then we walk for about 50 meters until we reach the Monte Grighini quartz dyke.

#### Stop 1.4 - The hugequartz dyke ( $8^{\circ}48'50.70''\text{E}$ - $39^{\circ}56'20.89''\text{N}$ )

The big quartz dyke is one of the most characteristic features of the Monte Grighini Complex, being visible, with its whitish color, from several kilometers away. The Monte Grighini quartz dyke is a massive, NE-SW-oriented dyke (Fig. 12a) of about 1.2-1.3 km in length and ~50-60 m in thickness. It belongs to a late Variscan dyke system, which in turn belongs to the Monte Grighini Intrusive Complex (Musumeci *et al.*, 2015), consisting of quartz-dykes, quartz-plagioclase-porphyry dykes, and aplite and pegmatite dykes hosted in the Monte Grighini Unit. The dykes crosscut the lithological contacts and tectonic structures (including the shear zone) and strike mainly orthogonal or parallel to the shear zone. The quartz dyke of this stop runs along the western slope of the mountain, and crosscut, from the top to the bottom, the metapelites of the Toccori Fm. and the monzogranites and leucogranites of the Intrusive Complex. The dyke reaches a maximum altitude of 670 m a.s.l. at the top of Monte Grighini, whereas, at the lowest altitude, the outcrop ends at ~370m a.s.l. near to Nuraghe Maiori locality. Approximately in its middle to lower part, when it encounters the monzogranites, the dyke is cut and shifted for ~40-50m by two subparallel, NW-SE-oriented faults. Looking at the SW direction (i.e. at the same direction of the quartz dyke towards the valley), the panoramic view from this stop shows a wide vegetative cover over the leucogranite/monzogranite bodies and, even more downstream, the late Variscan ultramylonite and cataclasite zones are visible. Towards NW we have a panoramic view of the top of Cuccuru Mannu (539 m a.s.l.) made up of leucogranites and, on its southern flank, we can have a look at the flat surface consisting of the sandstones and quartzite sandstones of Lower Eocene age belonging to the Monte Cardiga Fm. (Fig. 12b).

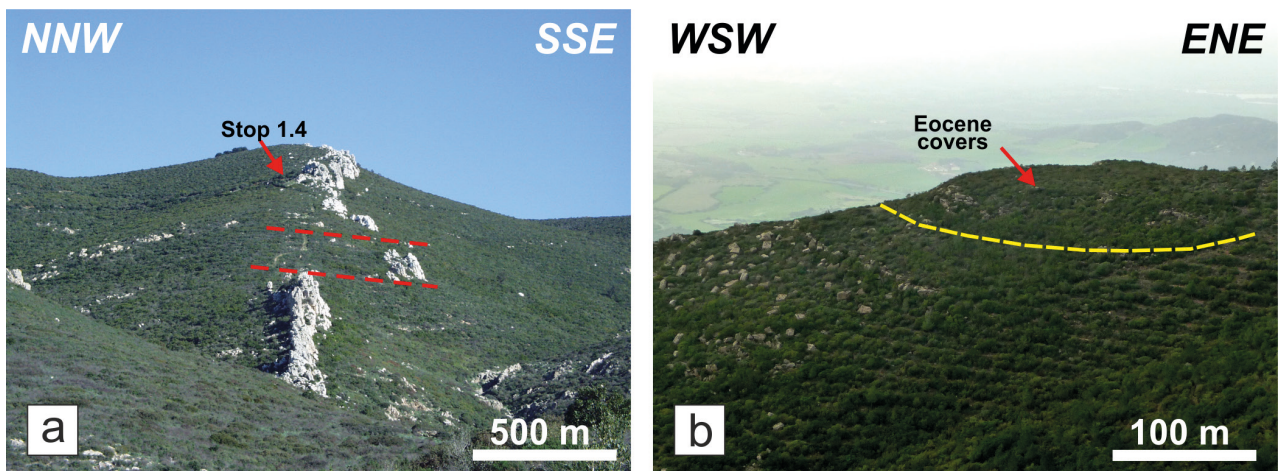


Fig. 12 - a) Monte Grighini quartz dyke seen from SW; b) Eocene covers at NW of the quartz dyke.

From Stop 1.4 we move towards N-NW for approximately 600 m and park near to a hut. We proceed by foot for other 350 m and arrive to the Cuccuru Mannu leucogranites.

**Stop 1.5 - Cuccuru Mannu leucogranites (8°48'36.27" E 39°56'42.96"N)**

The Monte Grighini leucogranites, that belong to S-type peraluminous suite of the late Variscan Intrusive Complex, crop out as a NW-SE elongated intrusion running along the whole Monte Grighini Unit. They are usually in contact with monzogranites in the central and northern part of the Complex (Fig. 13) and with the Toccori metapelites and ultramylonite/cataclasite zones in the southern part. Fine-grained, muscovite-bearing leucogranites characterized by the mineral assemblage Qtz + Kfs + Pl + K-Wmca ± Bt ± Grt host an hectometer-wide metapelite lens of the Toccori Fm.

In this outcrop (Figs. 6, 7) the leucogranites are characterized by protomylonitic to mylonitic fabric with well-developed C-type shear bands and S-C planes (Musumeci *et al.*, 2015). The C-type shear bands are marked by a continuous foliation (S-plane) with shape-preferred orientation of igneous minerals, cross-cut at low angle (<30°) by thin millimeter-spaced shear planes, known as C-planes (Fig. 14a, b). Close to the shear zone (towards SW), the S-planes progressively turn and become parallel to the C-planes. When the

ultramylonite zone is reached the two planes become parallel and only one foliation is observed.

The mean age of 298±2Ma for leucogranite emplacement, obtained with the Rb/Sr method on muscovite, is similar to the Ar/Ar age of 302±0.24Ma obtained on the same mineral (Del Moro *et al.*, 1991b). An undeformed leucogranite dyke outside the shear zone yielded an Rb/Sr muscovite age of 305±6Ma and Ar/Ar muscovite age of 296±1.5Ma (Musumeci, 1991a).

From this stop, looking towards SE, we take a panoramic look to the northern flank of Monte Grighini, where tonalite rocks belonging to the Intrusive Complex contains some lenses of dioritic rocks.

**Second day**

The second day of the field trip will be focused on the mylonitic granitoids that outcrop along the piedmont dirt road. It can be reached following the same driving directions of the first day until the left turn to Allai at the roundabout near Siamanna; after about 4 km along the S.P.39, turn on the right to a dirt road.

**Stop 2.1 - Riu S'Iscibi - mylonite-ultramylonite transition (8°47'54.44"E - 39°56'52.65"N)**

The Monte Grighini dextral, strike-slip shear zone runs along the southwestern and the southern sides of the complex (see Fig. 3). Shear strain, mainly partitioned in intrusive rocks, results in a mylonite - ultramylonite

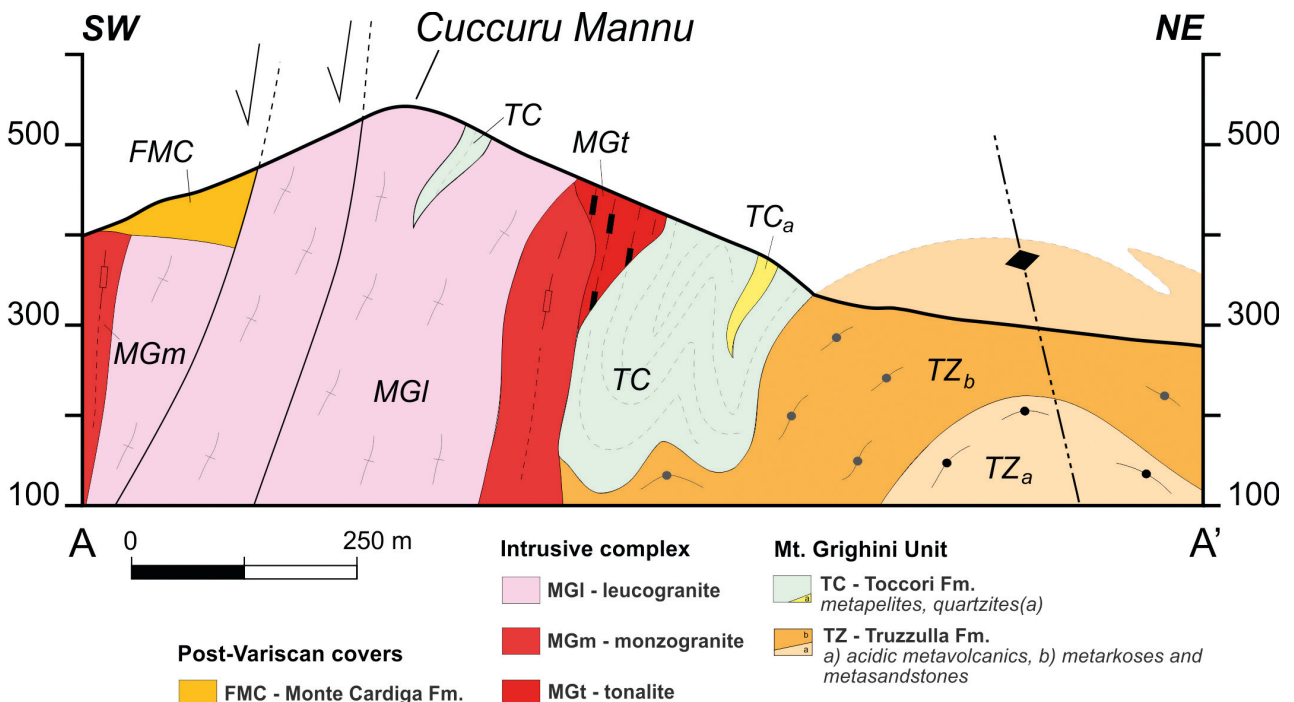


Fig. 13 - Geological cross section along the B-B' line of Fig. 3 (from Musumeci *et al.*, 2015, modified).

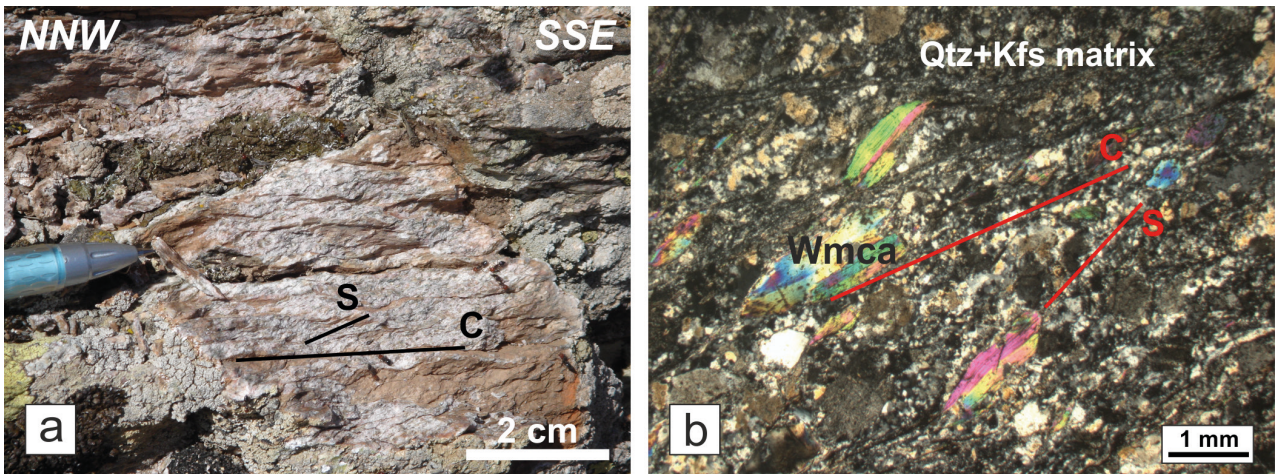


Fig. 14 - White mica-bearing leucogranite from Cuccuru Mannu. a) field photograph of S-C structures; b) photomicrograph of S-C structures, with mica-fish marking S planes.

sequence well exposed along the piedmont road cut. At Riu S'Ischibi (about 2 km after we left S.P.39; Figs. 6, 7) it is possible to observe a decameter-wide alternation of domains with different degree of shear deformation (Fig. 15a). Less deformed domains consist of coarse-grained monzogranites with S-C-type shear band that range from protomylonite to mylonite according to the porphyroclasts/matrix ratio (Wise *et al.*, 1984). Strain increase produces a decrease in grain size and the development of a pervasive mylonitic-ultramylonitic foliation, marked by millimeter thick quartz-rich layers with rare feldspar porphyroclasts and very thin phyllosilicate-rich layers. The highest degree of shear deformation is attained in correspondence of centimeter- to decimeter-thick, very fine-grained phyllonite layers. In thin section phyllonite are made up by very fine grained (5-10  $\mu\text{m}$ ) phyllosilicates where rare rounded quartz relics can be observed. Transition between strain domains is sharp and locally phyllonite can be in direct contact with protomylonite/mylonite rocks (Fig. 15a).

All domains are characterized by a pervasive foliation striking N150-160°, and dipping 65-75° to the WSW, with quartz mineral lineation gently to moderately plunging (10-25°) toward northwest.

Petrographic and microstructural observation highlights the mechanical and mineralogical processes affecting this sequence. Millimeter-sized, fractured K-feldspar porphyroclasts with domino-type and shear band-type structures occurring in the less deformed domains (Fig. 15b), are gradually reduced in grain size in high strain domains and are completely lacking in the highest strain domains (phyllonite fabric).

Phyllosilicates content tends to increase with deformation due to micas replacing feldspars according to a well known softening reaction (Hippertt & Hongn,

1998; Wibberley, 1999; Wintsch & Yeh, 2013 and references therein). Quartz concentrates in microcrystalline layers in all domains except in phyllonites, where it is dispersed in the matrix (Fig. 15c).

These processes were investigated by Columbu *et al.* (2015) through determination of petrophysical features of the different domains. The authors noticed that increasing deformation produce: (i) increase of solid density due to micas blastesis and feldspars breakdown; (ii) increase of total porosity due to the development of open intracrystalline and intrafoliar porosity; (iii) decrease of mechanical strength, especially along foliation planes, due to the strongly oriented micas and to the grain size decrease. "This changes of physical and mechanical properties allow strain and displacement to be partitioned into the weak shear zones" (Columbu *et al.*, 2015).

From previous stop we continue along the same road toward SE for about 1 km.

### Stop 2.2 - Phyllonite sequence (8°47'56.29"E - 39°56'39.13"N)

Moving toward SE the road cut exposes a decameter-thick sequence made up by ultramylonite-phyllonite sequence that represents the inner part of ultramylonite belt (Figs. 6, 7). These yellowish-brown rocks show a very fine-grained, foliated fabric where at the naked eyes it is possible to distinguish rare sub-millimeter-sized rounded porphyroclasts. As a consequence of the intense grain size reduction and absence of less deformed protomylonite-mylonite domains, as observed in the previous stop, these rocks locally may appear in the field similar to the low grade schist belonging to the nearby Gerrei Unit (Fig. 16a).

Well developed foliation strikes N130°, and dips 75° to the SW. The stretching lineation trends N120° and

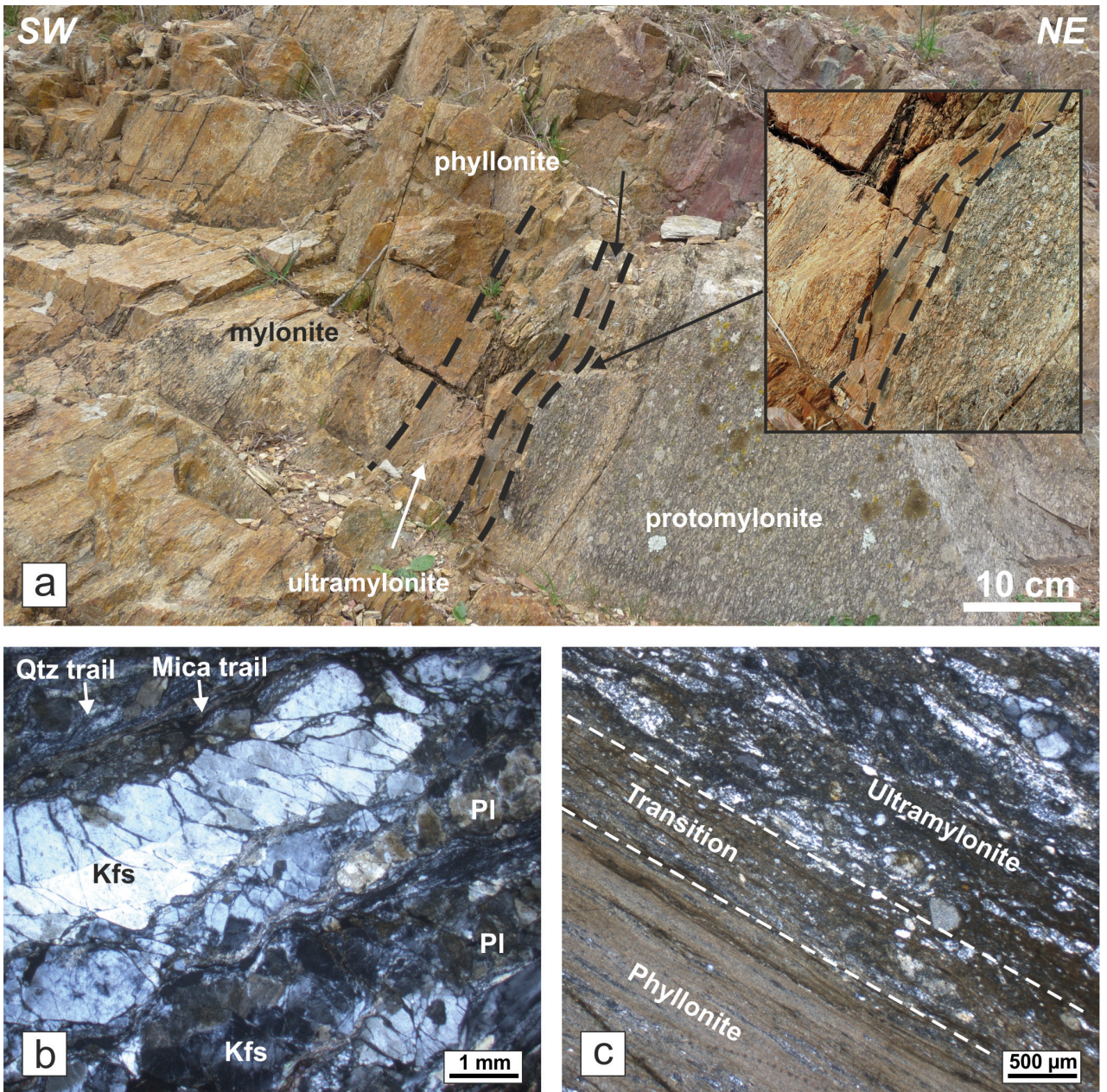


Fig. 15 - a) Representative sequence of the different strain domains; in the box, a detail of the sharp transition between protomylonite and phyllonite (from Columbu *et al.*, 2015, modified); b) photomicrograph of protomylonite showing large, fractured K-feldspar porphyroclasts and smaller, altered plagioclase surrounded by fine-grained matrix consisting of recrystallized quartz levels and mica trails; c) ultramylonite and phyllonite separated by a 1 mm thick transition belt.

plunges  $15^{\circ}\text{NW}$ . Locally, late, open folds with NE dipping axial planes are also observed (Fig. 16b). Microscopic observation shows millimeter-thick alternations of very fine-grained quartz-feldspathic-rich and mica-rich layers. Fine-grained K-feldspar porphyroclasts (100-200 mm) are concentrated along thin trails or, more rarely, dispersed in the matrix.

From Stop 2.2 we move toward SE for about 1 km until a farmhouse.

**Stop 2.3-Eocene covers ( $8^{\circ}48'07.16''\text{E}$ - $39^{\circ}56'11.03''\text{N}$ )** Monte Grighini Complex is surrounded by Eocene to Pliocene deposits. In this stop a Oligo-Miocene deposit belonging to the Ussana Fm. is exposed

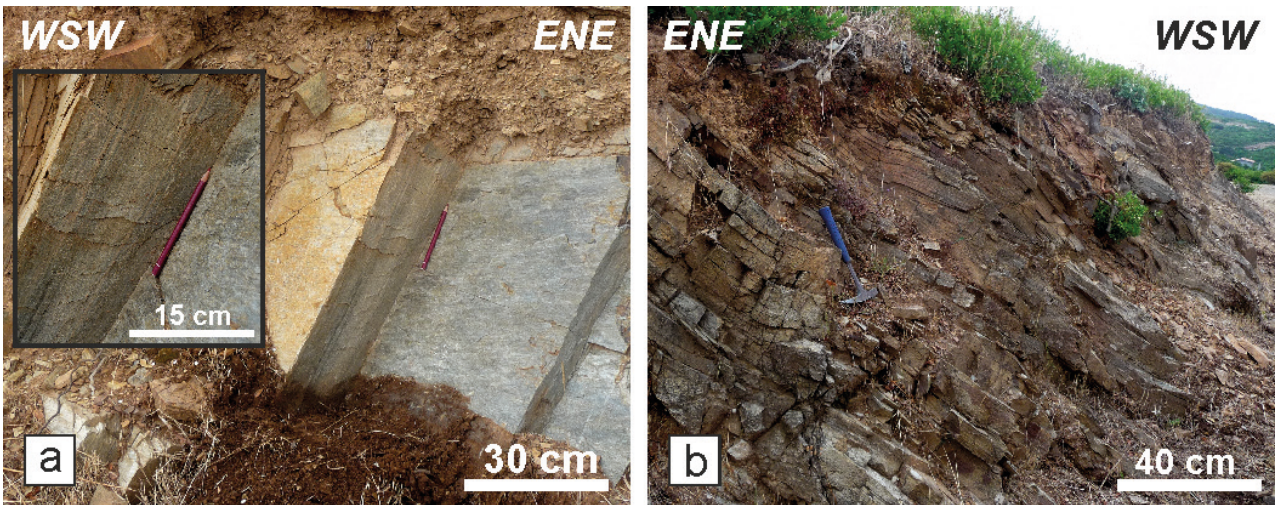


Fig. 16 - a) Ultramylonite outcrop characterized by very fine grain and pervasive foliation; b) open, late fold in ultramylonites.



Fig. 17 - a) Overview of the Oligo-Miocene sedimentary covers; b) close-up of the coarse, poorly sorted, sandy matrix.

(Figs. 6, 7). Ussana Fm. consists of poorly-sorted, sandy-clayey, reddish matrix with heterometric, polygenic (mainly metamorphics belonging to Paleozoic basement) clasts, ranging in size from pebbles to boulders.

It is considered a continental formation showing a complete facies transition from proximal colluvial fan to distal alluvial fan and braided river systems (Longhitano *et al.*, 2015). Ussana Fm. has been related to the



Fig. 18 - a) Lozenge-shaped structure, showing a faint foliation, within cataclasite; b) faulted aplite dyke in cataclasite.

opening of the Sardinian rift, that could represent the eastern branch of a complex rift system, linked to the opening of the Balearic basin (Cherchi & Montandert, 1982a,b).

In this outcrop (Fig. 17a), firstly reported by Assorgia *et al.* (1995), the Ussana Fm. consists of a matrix-supported assemblage with polygenic, poorly-sorted, clasts ranging in size from few centimeter to some decimeter. Matrix is a coarse-grained and quite mature (i.e. quartz- and feldspar- rich) sand. Clasts are commonly subrounded to rounded, suggesting their transport before sedimentation. The visible part of the outcrop does not show stratification or bedding, on the contrary it appears massive and chaotic (Fig. 17b). The above described features are similar to those of “facies 3b” of Longhitano *et al.* (2015), ascribed to an alluvial fan system.

From stop 2.3 we move toward SE along the same dirt road for less than 1 km.

#### **Stop 2.4 - Cataclasite zone (8°48'13.19"E - 39°55'55.30"N)**

The Monte Grighini shear zone is characterized by de-

tachment fault marked by a meter to decameter-thick cataclasite zone cropping out along the whole SW side of the complex. The cataclasite is in contact with the overlying low-grade metasediments and metavolcanics of Gerrei Unit. In this stop (Figs. 6, 7) a cataclasite zone is present. This cataclastic zone is mainly made up of intensely fractures and cataclastic rocks belonging to the Monte Grighini Unit, to the Gerrei Unit and to late Carboniferous granitoids. These rocks show several shear planes with different orientations; the prevailing shear surfaces strike N30-50° and dip 20-35° to the NW, whereas minor antithetic faults strike NS and dip 20-30° to the E. Locally, the NW dipping shear planes form lozenge-shaped structures (Fig.18a) where it is possible to recognize old foliations with variable orientations (from N50°-65°NW to N10°-65°W). Moving toward SE, massive, quartz-rich rocks occur, likely representing quartzite boulders within cataclasite. Proceeding along the same direction thin phyllonite levels occur, marking the transition from cataclasite to ultramyylonite belt. Within cataclasite quartz-feldspathic, non-foliated dykes, commonly affected by minor faults, are observed (Fig. 18b).

## ACKNOWLEDGMENTS

The authors greatly appreciated the comments of two anonymous reviewers that helped to improve the manuscript. Financial support was provided by Università di Cagliari and by FdS-RAS funding F72F16003080002.

## REFERENCES

- ASSORGIA A., BARCA S., FLORE G., LONIS R., LUXORO S.S., PINNA M., PORCU A., SECCHI F., SPANO C., 1995. Carta geologica del settore vulcanico e sedimentario Cenozoico compreso tra Fordongianus e Sini (Sardegna Centrale). Scala 1:50000. S.E.L.C.A. Ed., Firenze.
- BARCA S., CARMIGNANI L., ELTRUDIS A., FRANCESCHELLI M., 1995. Origin and evolution of the Permian-Carboniferous basin of Mulargia Lake (South-Central Sardinia, Italy) related to the Late-Hercynian extensional tectonics. *Comptes rendus de l'Académie des sciences. Série 2. Sciences de la terre et des planètes* 321(2): 171-178.
- CARMIGNANI L., CAROSI R., DI PISA A., GATTIGLIO M., MUSUMECI G., OGGIANO G., PERTUSATI P.C., 1994. The Hercynian chain in Sardinia. *Geodynamica Acta* 7: 31-47.
- CARMIGNANI L., CHERCHI G.P., DEL MORO A., FRANCESCHELLI M., GHEZZO C., MUSUMECI G., PERTUSATI P.C., 1987. The mylonitic granitoids and tectonic units of the Monte Grighini complex (Western-Central Sardinia): A preliminary note. In Sassi F., Bourrouilh R. (Eds), IGCP project N°8, 5. Correlation of variscan and pre-Variscan events of the Alpine-Mediterranean Mountain belt Newsletter: 25-26.
- CARMIGNANI L., COCOZZA T., GHEZZO C., PERTUSATI P.C., RICCI C.A., 1982. Lineamenti del basamento sardo. In: Guida alla geologia del Paleozoico sardo. Guide geologiche regionali. *Società Geologica Italiana*: 11-23.
- CARMIGNANI L., OGGIANO G., BARCA S., CONTI P., ELTRUDIS A., FUNEDDA A., PASCIS S., SALVADORI I., 2001. Geologia della Sardegna. Note illustrative della Carta Geologica della Sardegna in scala 1:200,000. *Memorie descrittive della Carta Geologica d'Italia LX*. 283 pp.
- CAROSI R., CRUCIANI G., FRANCESCHELLI M., MONTOMOLI C., 2015. The Variscan Basement in Sardinia. Field guide to the excursion of the 29<sup>th</sup> Himalaya-Karakoram-Tibet Workshop, 5-8 September 2014. *Geological Field Trips* vol. 7: 114 pp.
- CAROSI R., FRASSI C., IACOPINI D., MONTOMOLI C., 2005. Post collisional transpressive tectonics in northern Sardinia (Italy). *Journal of the Virtual Explorer* 19: 1-30.
- CAROSI R., MONTOMOLI C., TIEPOLO M., FRASSI C., 2012. Geochronological constraints on post-collisional shear zones in the Variscides of Sardinia (Italy). *Terra Nova* 24: 42-51.
- CAROSI R., MUSUMECI G., PERTUSATI P.C., 1990. Le Unità di Castello Medusa e Monte Grighini (Sardegna centro-meridionale) nell'evoluzione tettonica del basamento ercinico. *Bollettino della Società Geologica Italiana* 109: 643-654.
- CAROSI R., OGGIANO G., 2002. Transpressional deformation in northwestern Sardinia (Italy): insights on the tectonic evolution of the Variscan Belt. *Comptes Rendus Geoscience* 334: 287-294.
- CAROSI R., PALMERI R., 2002. Orogen parallel tectonic transport in the Variscan belt of northeastern Sardinia (Italy): implications for exhumation of medium-pressure metamorphic rocks. *Geological Magazine* 139: 497-511.
- CASINI L., OGGIANO G., 2008. Late orogenic collapse and thermal doming in the northern Gondwana margin incorporated in the Variscan Chain: A case study from the Ozieri Metamorphic Complex, northern Sardinia, Italy. *Gondwana Research* 13: 396-406.
- CASINI L., CUCCURU S., MAINO M., OGGIANO G., TIEPOLO M., 2012. Emplacement of the Arzachena Pluton (Corsica-Sardinia Batholith) and the geodynamics of incoming Pangaea. *Tectonophysics* 544-545: 31-49.
- CASINI L., CUCCURU S., PUCCINI A., OGGIANO G., ROSSI P.H., 2015. Evolution of the Corsica-Sardinia Batholith and late-orogenic shearing of the Variscides. *Tectonophysics* 646: 65-78.
- CHERCHI A., MONTANDERT L., 1982a. Oligo-Miocene rift of Sardinia and the early history of the western Mediterranean basin. *Nature* 298: 736-739.
- CHERCHI A., MONTADERT L., 1982b. Il sistema di rifting oligo-miocenico del Mediterraneo occidentale e sue conseguenze paleogeografiche sul Terziario sardo. *Memorie della Società Geologica Italiana* 24: 387-400.
- CHERCHI G., MUSUMECI G., 1987. Il leucogranito del M. Grighini (Sardegna centro-occidentale), un esempio di granito deformato all'interno di una fascia di taglio duttile: Caratteristiche meso e microstrutturali. *Atti della Società Toscana di Scienze Naturali Memorie XCIII*: 13-29.
- COLUMBU S., CRUCIANI G., FANCELLO D., FRANCESCHELLI M., MUSUMECI G., 2015. Petrophysical properties of a granite-protomylonite-ultramylonite sequence: insight from the Monte Grighini shear zone, central Sardinia, Italy. *European Journal of Mineralogy* 27(4): 471-486.
- CONNOLLY J.A.D., MEMMI I., TROMMSDORFF V., FRANCESCHELLI M., RICCI C.A., 1994. Forward Modelling of Ca-silicate microinclusion and fluid evolution in a graphitic metapelites (NE Sardinia). *American Mineralogist* 79: 960-972.
- CONTI P., CARMIGNANI L., FUNEDDA A., 2001. Change of nappe transport direction during the Variscan collisional evolution of central-southern Sardinia (Italy). *Tectonophysics* 332: 255-273.
- CONTI P., FUNEDDA A., CERBAI N., 1998. Mylonite development in the Hercynian basement of Sardinia (Italy). *Journal of Structural Geology* 20(2-3): 121-133.
- CORSINI M. & ROLLAND Y., 2009. Late evolution of the southern European Variscan belt: Exhumation of the lower crust in a context of oblique convergence. *Comptes Rendus Geoscience* 341: 214-223.
- CORTESOGNO L., GAGGERO L., OGGIANO G., PAQUETTE J.-L., 2004. Different tectono-thermal evolutionary paths in eclogitic rocks from the axial zone of the Variscan Chain in Sardinia (Italy) compared with the Ligurian Alps. *Ophioliti* 29(2): 125-144.
- COSTAMAGNA L.G., 2015. The Capo Malfatano Metaconglomerates in the Early Cambrian of SW Sardinia, Italy: key level for a new stratigraphic setting and evidence of Cadomian tectonics. *Zeitschrift der Deutschen Gesellschaft für Geowissenschaften* 166(1): 21-33.
- COSTAMAGNA L.G., ELTER F.M., GAGGERO L., MANTOVANI F., 2016. Contact metamorphism in Middle Ordovician arc rocks (SW Sardinia, Italy): New paleogeographic constraints. *Lithos* 264: 577-593.
- CRUCIANI G., DINI A., FRANCESCHELLI M., PUXEDDU M., UTZERI D., 2010. Metabasite from the Variscan belt in NE Sardinia,

- Italy: within-plate OIB-like melts with very high Sr and low Nd isotope ratios. *European Journal of Mineralogy* 22: 509-523.
- CRUCIANI G., FANCELLO D., FRANCESCHELLI M., SCODINA M., SPANO M.E., 2014a. Geothermobarometry of Al-silicate-bearing migmatites from the Variscan chain of NE Sardinia, Italy: a P-T pseudosection approach. *Periodico di Mineralogia* 83: 19-40.
- CRUCIANI G., FRANCESCHELLI M., ELTER F.M., PUXEDDU M., UTZERI D., 2008a. Petrogenesis of Al-silicate-bearing trondhjemitic migmatites from NE Sardinia, Italy. *Lithos* 102: 554-574.
- CRUCIANI G., FRANCESCHELLI M., FOLEY S.F., JACOB D.E., 2014b. Anatectic amphibole and restitic garnet in Variscan migmatite from NE Sardinia, Italy: insights into partial melting from mineral trace elements. *European Journal of Mineralogy* 26: 381-395.
- CRUCIANI G., FRANCESCHELLI M., GROppo C., 2011. P-T evolution of eclogite-facies metabasite from NE Sardinia, Italy: insights into the prograde evolution of Variscan eclogites. *Lithos* 121: 135-150.
- CRUCIANI G., FRANCESCHELLI M., GROppo C., OGGIANO G., SPANO M.E., 2015a. Re-equilibration history and P-T path of eclogites from Variscan Sardinia, Italy: a case study from the medium-grade metamorphic complex. *International Journal of Earth Sciences* 104: 797-814.
- CRUCIANI G., FRANCESCHELLI M., GROppo C., SPANO M.E., 2012. Metamorphic evolution of non-equilibrated granulitized eclogite from Punta de li Tulchi (Variscan Sardinia) determined through texturally controlled thermodynamic modelling. *Journal of Metamorphic Geology* 30: 667-685.
- CRUCIANI G., FRANCESCHELLI M., JUNG S., PUXEDDU M., UTZERI D., 2008b. Amphibole-bearing migmatite from Variscan Belt of NE Sardinia, Italy: partial melting of a mid-Ordovician igneous source. *Lithos* 102: 208-224.
- CRUCIANI G., FRANCESCHELLI M., LANGONE A., PUXEDDU M., SCODINA M., 2015b. Nature and Age of pre-Variscan eclogite protoliths from the Low- to Medium-Grade Metamorphic Complex of north-central Sardinia (Italy) and comparisons with coeval Sardinian eclogites in the northern Gondwana context. *Journal of the Geological Society* 172: 792-807.
- CRUCIANI G., FRANCESCHELLI M., MASSONNE H.-J., CAROSI R., MONTOMOLI C., 2013a. Pressure temperature and deformational evolution of high pressure metapelites from Variscan NE Sardinia, Italy. *Lithos* 175-176: 272-284.
- CRUCIANI G., FRANCESCHELLI M., MASSONNE H.-J., MUSUMECI G., SPANO M.E., 2016. Thermomechanical evolution of the high-grade core in the nappe zone of Variscan Sardinia, Italy: the role of shear deformation and granite emplacement. *Journal of metamorphic Geology* 34: 321-342.
- CRUCIANI G., FRANCESCHELLI M., MUSUMECI G., SPANO M.E., TIEPOLO M., 2013b. U-Pb zircon dating and nature of meta-volcanics and metakoses from the Monte Grighini Unit: new insights on Late Ordovician magmatism in the Variscan belt in Sardinia, Italy. *International Journal of Earth Sciences* 102: 2077-2096.
- CRUCIANI G., MONTOMOLI C., CAROSI R., FRANCESCHELLI M., PUXEDDU M., 2015c. Continental collision from two perspectives: a review of Variscan metamorphism and deformation in northern Sardinia. *Periodico di Mineralogia* 84: 1-44.
- DELAPERRIÈRE E., LANCELOT J., 1989. Datation U-Pb sur Zircons de l'orthognéiss du Capo Spartivento (Sardaigne, Italie), nouveau témoin d'un magmatisme alcalin ordovicien dans le Sud de l'Europe. *Comptes Rendus de l'Académie des Sciences de Paris* 309: 835-842.
- DEL MORO A., DI PISA A., OGGIANO G., VILLA I.M., 1991a. Isotopic ages of two contrasting tectono-metamorphic episodes in the Variscan chain in northern Sardinia. In: Cappelli B., Liotta D. (Eds), *Geologia del Basamento Italiano*: 33-35.
- DEL MORO A., LAURENZI M., MUSUMECI G., PARDINI G., 1991b. Rb/Sr and Ar/Ar chronology of Hercynian Mt. Grighini intrusive and metamorphic rocks (central-western Sardinia). *Plinius* 4: 121-122.
- DI VINCENZO G., CAROSI R., PALMERI R., 2004. The relationship between tectono-metamorphic evolution and argon isotope records in white mica: constraints from in situ <sup>40</sup>Ar-<sup>39</sup>Ar laser analysis of the Variscan basement of Sardinia. *Journal of Petrology* 45: 1013-1043.
- ELTER F.M., FAURE M., GHEZZO C., CORSI B., 1999. Late Hercynian shear zones in northeastern Sardinia (Italy). *Géologie de la France* 2: 3-16.
- ELTER F.M., MUSUMECI G., PERTUSATI P.C., 1990. Late Hercynian shear zones in Sardinia. *Tectonophysics* 176: 387-404.
- ELTER F.M., PANDELI E., 2005. Structural-Metamorphic Correlations Between Three Variscan Segments In Southern Europe: Maures Massif (France), Corsica(France)-Sardinia(Italy), And Northern Appennines (Italy). *Journal of the Virtual Explorer* 19 paper 5.
- ELTER F.M., PADOVANO M., KRAUS R.K., 2010. The emplacement of Variscan HT metamorphic rocks linked to the interaction between Gondwana and Laurussia: structural constraints in NE Sardinia (Italy). *Terra Nova* 22: 369-377.
- FERRARA G., RICCI C.A., RITA F., 1978. Isotopic ages and tectono-metamorphic history of the metamorphic basement of north-eastern Sardinia. *Contribution to Mineralogy and Petrology* 68(1): 99-106.
- FETTES D., DESMONS J. 2007. *Metamorphic Rocks – A Classification and Glossary of Terms*. Cambridge University Press, Cambridge, 244 pp.
- FRANCESCHELLI M., CARCANGIU G., CAREDDA A.M., CRUCIANI G., MEMMI I., ZUCCA M., 2002. Transformation of cumulate mafic rocks to granulite and re-equilibration in amphibolite and greenschist facies in NE Sardinia, Italy. *Lithos* 63: 1-18.
- FRANCESCHELLI M., MEMMI I., RICCI C.A., 1982. Ca distribution between garnet and plagioclase in pelitic and psammitic schists from the metamorphic basement of north eastern Sardinia. *Contributions to Mineralogy and Petrology* 80: 285-295.
- FRANCESCHELLI M., PUXEDDU M., CRUCIANI G., 2005a. Variscan metamorphism in Sardinia, Italy: review and discussion. In: Carosi R., Dias R., Iacopini D., Rosenbaum G. (Eds), *The southern Variscan belt. Journal of the Virtual Explorer, Electronic Edition* 19: Paper 2.
- FRANCESCHELLI M., PUXEDDU M., CRUCIANI G., DINI A., LOI M., 2005b. Layered amphibolite sequence in NE Sardinia, Italy: remnant of a pre-Variscan mafic silicic layered intrusion? *Contributions to Mineralogy and Petrology* 149: 164-180.
- FRANCESCHELLI M., PUXEDDU M., CRUCIANI G., UTZERI D., 2007. Metabasites with eclogite facies relics from Variscides in Sardinia, Italy: a review. *International Journal of Earth Sciences* 96: 795-815.
- GAGGERO L., OGGIANO G., FUNEDDA A., BUZZI L., 2012. Rifting and arc-related early Paleozoic volcanism along the north

- Gondwana margin: geochemical and geological evidence from Sardinia (Italy). *The Journal of Geology* 120: 273-292.
- GHEZZO C., MEMMI I., RICCI C.A., 1979. Un evento granulitico nel basamento metamorfico della Sardegna nordorientale. *Memoirie della Società Geologica Italiana* 20: 23-38.
- GIACOMINI F., BOMPAROLA R.M., GHEZZO C., 2005. Petrology and geochronology of metabasites with eclogite facies relics from NE Sardinia: constraints for the Palaeozoic evolution of Southern Europe. *Lithos* 82: 221-248.
- HELBING H., 2003. No suture in the Sardinian Variscides: a structural, petrological and geochronological analysis. *Tübinger Geowissenschaftliche Arbeiten Reihe A* 68. 190 pp.
- HIPPERTT J.F., HONGN F.D., 1998. Deformation mechanisms in the mylonite/ultramylonite transition. *Journal of Structural Geology* 20(11): 1435-1448.
- JUNKER B., SCHNEIDER H.H., 1983. The Infracambrian Bithia Formation - its facies development in Southwest Sardinia. *Neues Jahrbuch für Geologie und Paläontologie Monatshefte* 24: 369-384.
- LAURENZI M.A., DEL MORO A., MUSUMECI G., PARDINI G., 1991. Rb/Sr and Ar/Ar chronology of Monte Grighini intrusive Complex (Sardinia, Italy). *Terra Abstract* 3: 501-502.
- LONGHITANO S.G., SABATO L., TROPEANO M., MURRU M., CARRANNANTE G., SIMONE L., CILONA A., VIGORITO M., 2015. Outcrop reservoir analogous and porosity changes in continental deposits from an extensional basin: The case study of the upper Oligocene Sardinia Graben System, Italy. *Marine and Petroleum Geology* 67: 439-459.
- MARTINI I.P., TONGIORGI M., OGGIANO G., COCOZZA T., 1991. Ordovician alluvial fan to marine shelf transition in SW Sardinia, Western Mediterranean Sea: tectonically ("Sardic phase") influenced clastic sedimentation. *Sedimentary Geology* 72(1-2): 97-115.
- MASSONNE H.-J., CRUCIANI G., FRANCESCHELLI M., 2013. Geothermobarometry on anatectic melts - a high-pressure Variscan migmatite from northeast Sardinia. *International Geology Review* 55: 1490-1505.
- MILLER C., SASSI F.P., ARMARI G., 1976. On the occurrence of altered eclogitic rocks in north-eastern Sardinia and their implication. *Neues Jahrbuch für Geologie und Paläontologie Monatshefte* 11: 683-689.
- MUSUMECI G., 1991a. Tettonica trascorrente, magmatismo e metamorfismo nel basamento ercinico sardo: il Complesso del Monte Grighini (Sardegna centro-occidentale). Unpublished PhD dissertation, Università di Pisa (Italy). 287 pp.
- MUSUMECI G., 1991b. Displacement calculation in a ductile shear zone: Monte Grighini shear zone (Central-Western Sardinia). *Bollettino Società Geologica Italiana* 110: 771-777.
- MUSUMECI G., 1992. Ductile wrench tectonics and exhumation of hercynian metamorphic basement in Sardinia: Monte Grighini Complex. *Geodinamica Acta* 5(1-2): 119-133.
- MUSUMECI G., SPANO M.E., CHERCHI G.P., FRANCESCHELLI M., PERTUSATI P.C., CRUCIANI G., 2015. Geological map of the Monte Grighini Variscan Complex (Sardinia, Italy). *Journal of Maps* 11: 287-298.
- OGGIANO G., GAGGERO L., FUNEDDA A., BUZZI L., TIEPOLO M., 2010. Multiple early Paleozoic volcanic events at the northern Gondwana margin: U-Pb age evidence from the southern Variscan branch (Sardinia, Italy). *Gondwana Research* 17(1): 44-58.
- PADOVANO M., ELTER F.M., PANDELI E., FRANCESCHELLI M., 2012. The East Variscan Shear Zone: new insights into its role in the Late Carboniferous collision in southern Europe. *International Geology Review* 54: 957-970.
- PALMERI R., FANNING M., FRANCESCHELLI M., MEMMI I., RICCI C.A., 2004. SHRIMP dating of zircons in eclogites from the Variscan basement in north-eastern Sardinia (Italy). *Neues Jahrbuch für Mineralogie Monatshefte* 2004(6): 275-288.
- PAVANETTO P., FUNEDDA A., NORTHRUP C.J., SCHMITZ M., CROWLEY J., LOI A., 2012. Structure and U-Pb zircon geochronology in the Variscan foreland of SW Sardinia, Italy. *Geological Journal* 47: 426-445.
- PILLOLA G.L., 1991. Trilobites du Cambrien inférieur du SW de la Sardaigne, Italie. *Palaeontographia Italica* 78: 1-173.
- RICCI C.A., CAROSI R., DI VINCENZO G., FRANCESCHELLI M., PALMERI R., 2004. Unravelling the tectono-metamorphic evolution of medium-pressure rocks from collision to exhumation of the Variscan basement of NE Sardinia: a review. Special issue 2: a showcase of the Italian research in metamorphic petrology. *Periodico di Mineralogia* 73: 73-83.
- SCHNEIDER J., CORSINI M., REVERSO-PEILA A., LARDEAUX J.M., 2014. Thermal and mechanical evolution of an orogenic wedge during Variscan collision: an example in the Maures-Tanneron Massif (SE France). In: Schulmann K., Martinez Catalan J.R., Lardeaux J.M., Janousek V., Oggiano G. (Eds), The Variscan Orogeny: Extent, Timescale and the Formation of the European Crust. *Geological Society of London, Special Publications* 405: 313-331.
- WIBBERLEY C., 1999. Are feldspar-to-mica reactions necessarily reaction-softening processes in fault zones? *Journal of Structural Geology* 21(8): 1219-1227.
- WINTSCH R.P., YEH M.W., 2013. Oscillating brittle and viscous behavior through the earthquake cycle in the Red River Shear Zone: Monitoring flips between reaction and textural softening and hardening. *Tectonophysics* 587: 46-62.
- WISE D.U., DUNN D.E., ENGELDER J.T., GEISER P.A., HATCHER R.D., KISH S.A., ODOM A.L., SCHAMEL S., 1984. Fault-related rocks: Suggestions for terminology. *Geology* 12(7): 391-394.

(ms. pres. 28 aprile 2017; ult. bozze 20 settembre 2017)



Edizioni ETS  
Piazza Carrara, 16-19, I-56126 Pisa  
info@edizioniets.com - www.edizioniets.com  
Finito di stampare nel mese di dicembre 2017

